RUHR UNIVERSITÄT BOCHUM

RUHR-UNIVERSITÄT BOCHUM | 44801 Bochum | Germany

FAKULTÄT FÜR CHEMIE UND BIOCHEMIE

AG EPR-Spektroskopie
Gebäude NBCF 03/498
Universitätsstraße 150, 44801 Bochum

Prof. Dr. Enrica Bordignon
Fon +49 (0)234 32-26239

email : enrica.bordignon@rub.de

To the Editor of Magnetic Resonance

3. September 2020

Dear Editor,
Dear Prof. Prisner,

Please find enclosed the revised version of the manuscript entitled: 'Strategies to identify and suppress crosstalk signals in DEER experiments' by Markus Teucher, Mian Qi, Ninive Cati, Henrik Hintz, Adelheid Godt and Enrica Bordignon.

We thank both reviewers for their comments, which we addressed in the revised version.
The main changes are briefly summarized in the following:

1. We now provide a quantification of the crosstalk signals based on the relative intensities of the peaks in the distance distribution (new Table S5 in SI Part B).
2. Concerning the error estimation, we focused on the presence of distance peaks from the rulers present in the sample and did not highlight the uncertainties in the distance distributions. We agree that this should be done. Therefore, we provide now in all DEER figures in the main text (new Figs. 4-9) the distance uncertainties obtained via DeerNet, which we think is nowadays the most suitable approach to reliably obtain such errors.
3. We provide a detailed analysis of the nutation experiments performed to optimize the DEER channels for the different spin types and relaxation data on all rulers at different temperatures (new Fig. 2 and new Section 3 in the SI Part B).
4. We now exploit the potential of the swapped setup (new panel d in Fig. 3) that we previously suggested for the NOGd channel at higher temperatures. We found that 30 K is the best compromise to have a relatively short T1 of the observer nitroxide (fast acquisition time) and a relative long T1 (longer than the dipolar evolution time) of the pumped Gd spins. We found that this setup can suppress the crosstalk signal, although providing lower modulation depth and lower signal-to-noise than the conventional setup. Therefore, in the revised version, we provide not only a quick identification strategy for the Gd-Gd crosstalk signal in the NOGd DEER channel, but also a suppression strategy (new Fig. 9 and new Fig. S3 in the SI Part B).

5. We changed the title to introduce the new suppression strategy and we removed the term ‘orthogonal’, which, despite being used in literature, is clearly not completely adequate for nitroxide and gadolinium spins, based on the described crosstalk effects.

We think that the revised version increased the quality and clarity of the presented study, and we will be delighted to see this manuscript published in MR.

Finally, we would like to point out that some comments from anonymous reviewer 2 were inappropriate. According to COPE ethical guidelines for peer reviewers, the peer reviewers should be objective and constructive in their reviews, refraining from being hostile or inflammatory and from making libelous or derogatory personal comments.

Sincerely, on behalf of all authors

Prof. Dr. Enrica Bordignon
Ruhr-Universität Bochum
Germany

Point by point response to the Anonymous Referee #1

(in grey the comments of the ref #1, in black our responses)

This manuscript focuses on DEER distance measurements between Gd(III) and a nitroxide (NO) radical, often referred to as orthogonal spin labeling. One of the motivations for using such labeling schemes is the ability to carry out selective distance measurements, for example if a biomolecule is labeled with one NO and one Gd(III), then one can probe intra molecular distance via Gd-nitroxide and intermolecular distances (which can arise from oligomerization) by Gd(IIII)-Gd(III) or NO -NO distance measurements. This approach was introduced already in 2012 (DOI: 10.1039/C2CP40282C, Phys. Chem. Chem. Phys., 2012, 14, 10732-10746, which unfortunately is not referenced by the authors).

This approach was introduced before by the same pioneering authors (Lueders, Jeschke and Yulikov in 2011, https://doi.org/10.1021/jz200073h) which was already referenced. However, the suggested reference is added together with the first NO-Gd measurements from an independent group (Kaminker, PCCP 2012, DOI: 10.1039/c2cp40219j).

Other reasons maybe increased sensitivity compared to Gd(III)-Gd(III) and elimination of the effect of the dipolar pseudosecular terms on the DEER modulation frequencies in the case of short distances. In this work the authors used three model compounds with two NO, one NO and one Gd(III) and two Gd(III)-Gd(III) and use them to evaluate how selective are the Gd(III)-Gd(III), Gd(III)-NO and NO- NO distance measurements, while exploiting the different spectral and spin dynamics properties, which have been highlighted in earlier works. This work does not present any new original ideas but using well defined model compounds that can be mixed in a control manner they clearly show expected pitfalls and when they can be overcome and when not. These arise from the spectral overlap of Gd(III) and NO throughout the spectral width of the NO. The authors refer to the consequences of this overlap in various pulse set-ups for DEER as “cross talk”. The value of this manuscript is mainly “educational’ as it nicely highlights all issues involved in such measurements on controlled samples. The authors borrowed from optics the nomenclature of color channels to accompany their explanations and in the figs use the associated colors, which again has educational value. I think that after appropriate revisions following the comments below this manuscript will be of value to practitioners of DEER and therefore I recommend publication.

Thanks for the positive evaluation of our work. We agree that this work is educational, and it is meant to give a clear picture of the pitfalls that can be encountered when working with two non-perfectly orthogonal spin labels. In the revised version we added ‘non-perfectly orthogonal’ to the title, provided a quantification of the relative modulation depths and the uncertainties in the DEER data, a series of relaxation measurements at different temperatures and we developed an additional strategy to suppress the unwanted Gd-Gd crosstalk signals from the NOGd channel (swapped NOGd DEER setup at 30 K). We borrowed the terms ‘channel’ and ‘crosstalk’ from optics to simplify the description of the different DEER setups, and to avoid confusion between crosstalk signals, the already known 2+1 signals and possible artifacts in DEER traces.

1. In Fig. 3 the bandwidth of the pump and observe pulses are assumed to be the same but I think that this is incorrect, the bandwidth of an echo detection sequence (two or three pulses) is not the same as just that of the pi pulse. This is even mentioned by the authors (page 13, line 220). Please calculate the correct bandwidth and change Fig. 3.

In the setup used in this work we have all observer pulses with the same length (32 ns Gaussian), to avoid different excitation bandwidths by the pi/2 and pi pulses in the observer sequence. The excitation bandwidth is calculated with the Easyspin functions 'exciteprofile' (https://easyspin.org/easyspin/documentation/exciteprofile.html) and 'pulse' (https://easyspin.org/easyspin/documentation/pulse.html), which allow using different pulse shapes. 'exciteprofile' computes the excitation profiles for an input pulse function using two-level density matrix dynamics starting from thermal equilibrium (Mx = 0, My = 0, Mz = 1). The magnetization output cannot be used to continue density propagation, therefore we could not directly calculate the excitation profile of the three Gaussian pulses separated by the given interpulse delays. However, the presented excitation profile of the observer in Fig. 3 was used to aid the positioning of the observer and pump pulses to avoid overlap, and therefore the appearance of the 2+1 signal at the end of the time trace, as done in Teucher and Bordignon, JMR, 2018. In the legend of Fig. 3, we clarified further that the presented excitation profile is from one ideal Gaussian pi pulse, without taking into account the spectral function, the non-linearity of the signal response, the cavity profile or the Q factor.

2. The manuscript is very qualitative and its level can be increased by calculating the predicted modulation depth for NO and Gd(III) at the relevant pump frequencies and compare to the observations. As they have the full lineshape of the Gd(III) and the NO this can be easily done. Similarly, they can account for the degree of overlap for the observe sequence for the different conditions. Such calculations can actually serve to guide the experimental optimized set up. In table S2 the authors mention "Theoretically possible" but as they did not do any theoretical calculations, this term is inappropriate.

We followed your suggestion: we added a new supplementary table that contains an overview of the modulation depths and the relative populations of the individual distances (see Table S5, SI Part B). Concerning the calculation of expected modulation depths with Gd spins: this is not a trivial task since it was already shown that it is difficult to match the theoretical modulation depths for the GdGd channel with those experimentally detected (see Goldfarb, PCCP, 2014, 16, 9685−9699 and Manukovsky et al., J. Chem. Phys. 2017, 147 (1−9), No. 044201). Notably the modulation depths of the GdGd channel also depends on temperature and on the length of the traces (Gordon-Grossman et al., PCCP, 13(22):10771-80). Additionally, to take into account the crosstalk signals, we should consider the non-optimal excitation of the spins with different transition moments both in the observer and in the pump pulse. As a last complication, the pump pulse is placed at different positions within the resonator profile depending on the DEER setup (see Fig. 3) which also must be considered. Such calculations are out of the scope of this manuscript, and they would have a rather limited value for the practitioner since the strength of the crosstalk signal vs real signal is dependent on the chosen setup (pulse lengths, power, positioning) and on the relative ratio between the spin types present in the sample, therefore any quantification would be more or less unique for the system under study. We modified the 'theoretically possible' in the table with 'possible' based on the existing overlap between NO and Gd in the pump and/or observer positions.

3. The presentation of normalized distance distributions without the uncertainties evaluated by validations are misleading. For example, in Fig. 1c the trace is very noisy and the modulation depth is small, yet the distance distribution is nice and intense just like the one below. This is just one example but is occurs in many of the Figs. This should be corrected, the P(r) values should be noted on the Y axis and uncertainties should be shown. In Fig. S1 they show that there is no real difference between Gaussian and

Tikhonov regularization. So if they chose Tikhonov regularization this may be easier to show.

Thank you for this suggestion. Indeed, we focused on the presence of distance peaks from the rulers that we added in the sample and did not highlight the uncertainties in the distance distributions, which are however minor for most data presented. Now we provide the distance uncertainties obtained via DeerNet, that we think is nowadays the most suitable approach to reliably obtain such errors. In fact, the outcome of a Tikhonov or Gaussian validation is strongly dependent on the parameters set by the user, whilst the evaluation of the uncertainties in the DEER traces using DeerNet in DeerAnalysis2019 is unbiased. The neural network analysis is shown for all DEER experiments of the main text (Fig. 4 to 9) and we provide an additional figure (Fig. S9, SI Part B) showing the performance of different neural networks in finding crosstalk signals. Furthermore, we added, as suggested, the y-axis titles in the distance distributions. We kept the Gaussian analysis of the DEER data over Tikhonov since fitting the data using Gaussians allows quantification of the ratio between different peaks, which is now presented in the new Table S5 (SI Part B).

4. Why was the Gd(III) pulse taken as 24 ns, when there is enough power to shorten it and improve SNR.

In the NOGd DEER setup (Fig. 3(b)), the pump pulse on the NO was chosen to be a 24 ns Gaussian pulse (note that this is a 10.2 ns FWHM) and all Gaussian observer pulses were set to 32 ns (note that this is 13.6 ns FWHM). Currently, with this setup this is the maximally available power.

Indeed, the 32 ns pump and observer pulses used in the GdGd DEER setup at 100 MHz separation could be shortened, however, to avoid overlap of the pulses, this would require increasing the interpulse separation and moving the observer to a region of lower spectral density. We also did not want to increase the excitation bandwidth of the pump at the maximum of the Gd much further to avoid partial excitation of the NO spectrum (see Fig. 3(c)). This setup is therefore optimal for our spectrometer, and results in a crosstalk-free GdGd channel.

5. Please explain why you choose to add the Gd-Gd ruler in a twice as much concentration, is this to enhance the “cross talk”?

We clarified this issue in the text (e.g. first paragraph in section 3.2). Indeed, we chose two ratios to show the dependence of the appearance of the crosstalk signals on the relative spin concentrations. Different stoichiometric ratios can in fact be encountered in real experiments on biological systems. Most crosstalk signals appear in both stochiometric ratios but we also clarify that when the Gd-Gd ruler is present in excess (two-fold in this case), the crosstalk signal X_3 is visible, however if it is present in a 1:1 ratio, it

becomes negligible. The experiments with the three rulers in equimolar concentrations can be found in the SI Part B, Table S6 and Fig. S5-S7.

6. The spectrometer artifact is worrisome – it is larger than the cross talk. What is the source of the artifact and why it appears only in the red channel?

We also find this artifact very worrisome and tried multiple approaches to identify and suppress it. Unfortunately, to date without any success. We added a new Fig. S8 (SI Part B) in which DEER traces were measured on isolated maleimide Gd-DOTA labels in solution to show that this artifact is a sinusoidal oscillation which is mostly present in the imaginary part of the signal, it is independent of the dipolar frequency, it is not an ESEEM signal, and can be found also in solutions of $MnCl_2$, therefore Gd-independent.

7. P. 3 line 67: You should use TM (phase memory time) and not T2. Also the differences in phase memory time of Gd(III) and NO is not very different. If you know of cases where it has been used to filter NO and Gd(III) please give a ref.

Thank you for this remark. Indeed, the difference in T_m is not sufficient to filter NO and Gd, only T_1 can be used. Therefore, we removed this part of the sentence. Additionally, in the revised version of the paper we show a series of data on T_m and T_1 measured on different samples, at different spectral positions and at different temperatures (see new section 3 in SI Part B).

8. It is more appropriate to cite the original papers than a review. There are not so many examples of Gd(III) –nitroxide distance measurements so better give credit to the original papers and not a review.

We agree with your suggestion, therefore we added to our knowledge all references about DEER performed on different spin types.

9. In general the referencing is rather poor, focusing on self-citations. The omission of the work of Lovett is one example. Another one is the omission of distance measurements between three different spins (Gd(III), nitroxide and Mn(III) (Goldfarb group) and the reference mentioned at the beginning of this evaluation. P. 2 line 35 please give a reference to the DD software as well when mentioning Gaussian fits.

We had 5 references from our group over 45 references in total. However, we added more references (in particular, see section 1.2). The total number of references is now 65. The DD software is also cited among the possible methods to extract distance distributions (Stein et al., 2015).

10. Isn't the easiest way the identify the X2 and X3 crosstalk is just running a Gd(III)-Gd(III) set up and see that it is the same distance as observed in the cross talk.

Of course, we mention this possibility for the NO-Gd crosstalk signal in the NONO channel (X_1) but this strategy can be ambiguous on real biological systems. In this case it is straightforward, because we know which distances to expect in our samples, but this is not a situation generally found, and two channels can have very similar distance distributions.

11. Please shorten the conclusions – no reason to have a two-page conclusion that just repeat the results. Should be short and to the point.

We shortened the conclusions as suggested.

Point by point response to the Anonymous Referee #2

(in grey the comments of the ref #2, in black our responses)

Teucher et al. describe a systematic investigation of distance distribution artifacts that can occur in orthogonally spin-labelled biomacromolecules when specific spins cannot be exclusively addressed but the pulses also excite other spins unintentionally. There are no new concepts or experiment designs in this manuscript but the declared aim is to provide a strategy for identifying and possibly removing 'false positive' distance contributions. While the results do not bring many surprises, this could have been a worked example of how one can thoroughly identify and quantify these artifacts in the distance distribution. However, with the current lack of quantification and error estimation in the analysis this is almost entirely anecdotal with limited value to practitioners.

Once the artifacts are quantified and the most important avenues for their suppression explored and experimental uncertainties are given this may become publishable. In the current state publication would be premature.

We now provide a quantification of the crosstalk signals based on the relative intensities of the peaks in the distance distributions (see new Table S5, SI Part B) which is of course reflecting the given values of the modulation depths. We would like to highlight that such a quantification may be of limited value for practitioners as it is strongly dependent on the setup and on the samples used, therefore these numbers are more or less unique for the system under study.

Concerning the error estimation, we focused on the presence of distance peaks from the rulers present in the sample and did not highlight the uncertainties in the distance distributions. We agree that this should be done, and we provide now in all DEER figures in the main text (Fig. 4 to 9) uncertainties obtained via DeerNet, which we think is nowadays the most suitable approach to reliably obtain such errors.

We now exploit the potential of the swapped setup that we suggested in the NOGd channel at higher temperatures and found that indeed this setup can suppress the crosstalk signal. Therefore, we have not only identification but also suppression strategies in the new Fig. 9.

Model system

1 You find a much broader distance distribution of the NO-NO ruler than found for the homologous ester-inked structures. As this is unlikely to be rooted in real backbone flexibility (cf. Jeschke JACS 2010 cited in here) and acid amides will not be more flexible than esters either I would suspect a distribution in small exchange couplings. How does the fast motion cw EPR compare with ester-linked rulers? It seems odd to generate a new structure for this study and not fully investigate its spectroscopic properties.

Indeed, the NO-NO-ruler is a new compound, which was chosen because of its very small spin-spin distance which does not overlap with the mean distances of the other two available rulers. The reason for a smaller distance and a broader spin-spin distance distribution of the NO-NO ruler in comparison to structurally related NO-NO rulers with ester instead of amide linkages between the spacer and the nitroxide moiety is a consequence of the side chains at the N atoms. The experimentally found distance

agrees with the nitroxide moiety and the benzene ring being preferentially oriented trans with respect to the NH-CO bond (s-trans conformation). Adding a PEG chain to the N atom lifts this sterically founded preference and thus makes conformations with smaller dihedral angles accessible and energetically comparable. This reduces the spin-spin distance and broadens the distance distribution. Here, we are only interested in having at disposal a distinguishable short distance arising from a NO-NO ruler, however, a detailed analysis of the properties of a series of new rulers will be the subject of another manuscript.

DEER setup

2 You describe the experiments insufficiently to allow independent reproduction of the results. How were the power levels calibrated? You write reducing the AWG output from 100% to 22% corresponds to 12 dB attenuation. Is this frequency independent, is this with the TWT in saturation at 100%? With some of your results not showing the expected microwave power response it is important to understand how the settings were optimized and controlled. Were all pulse power levels optimized via nutation experiments at the respective frequencies to account for the limited resonator bandwidth? This is not clear from the current description. What are the expected differences in nutation between Gd and NO in the NONO and GdNO channels? The contribution from the central transition is not all out dominant at these pump frequencies.

We tried to describe the DEER experiments in a very detailed way as usual, including pulse lengths, types, positions with respect to the spectra, frequency separation, temperature, etc. We wrote 'The length of the pulses was optimized via transient nutation experiments for each spin type as shown in Fig. 2.' We did not describe deeply the standard procedure we use to set up the experiments via nutation, but the AWG amplitudes and shot repetition times shown in the old Fig. 2 should have exemplified this approach. Of course these numbers were not used as general values across all setups, in fact, as written, we optimized the pump and observer pulse lengths for each DEER setup, on each sample and for each spin type individually via transient nutation experiments to account for the different positions in the resonator dip and the limited resonator bandwidth.
We further clarified this aspect in the text by the addition of a new paragraph on nutation experiments (section 2.2.2) and an extension of Fig. 2 (see also Table S2, SI Part B). Fig. 2 shows now the changes in the Gd and NO nutation frequencies at different positions in the spectrum as a function of the main attenuator and the AWG amplitudes. These data illustrate also that the nutation frequencies were very similar when detected at the maximum of the Gd signal or 280 MHz higher in frequency, which indicates that the major contribution arises from the -1/2 to +1/2 transition.

Distance analysis

3 Increase the size of your figure panels. Six-panel wide figures with uniformly scaled distance distributions and DEER signals make it very hard to see the detail of the data. Many of the figures are only 3 panels wide with lots of white space around the data panels.

Thank you for this suggestion, we increased the figure and font sizes and added new panels with the DeerNet analysis.

4 Gaussian fitting does indeed allow a much more stable parametrized analysis. The comparison with Tikhonov Regularization must be extended to the pure rulers (Fig S3). None of the Gaussian fits is particularly good so that the model free analysis has to be shown.

The Tikhonov analysis was already shown for the pure rulers (in the suppl. Figure which is now Fig. S4) to compare the distance distributions with those obtained by Gaussian fit, how could we extend that?

We decided to add a model-free analysis using DeerNet in the main figures which also provides an uncertainty estimate to be compared with the Gaussian analysis. The results from both methods are in good agreement with each other. We kept the Gaussian analysis in the main figures since it allows for an extraction of the relative ratios of the different peaks in the distance distributions, which are now shown in the new Table S5 (SI Part B). Notably, the validation procedure is not available for the Gaussian analysis in DeerAnalysis2019.

5 Nevertheless, the Gaussian fits allow straightforward quantification of contributions of different distances to the modulation depth. This should be don't throughout and replace the qualitative discussion (see below). The GdGd ruler should contribute to the NONO channel. The signal may be too weak to detect but this should at least be mentioned here. Looking at the spectral overlap a contribution of the GdNO ruler to the NONO DEER does not seem "surprising" at all.

A quantification of the distance contributions based on the modulation depths was already present in the text. However, we now added a quantification based on the Gaussian fits which reflect the contributions of the modulation depths. A new table with all extracted parameters is now presented in the SI Part B (Table S5).

We already mentioned that a GdGd crosstalk signal in the NONO DEER channel was possible and classified it as X_4 (page 14 line 252 in the submitted manuscript and Table S2 in the original manuscript, now Table S7). We also discussed that it is probably too weak to be detected.

Modulation depths

6 NONO DEER gives 35% and NOGd 30%. You must provide error estimates. Is the difference significant? These are both synthetic rulers with 100% nitroxide labelling. One might assume the modulation depths should be identical unless you can give reasons for the opposite. This needs to be quantitatively addressed.

All mod. depths are now presented in Table S5 (SI Part B). When comparing the data presented in Fig. 4(c) and in Fig. S5, one can see that for an independent repetition (different sample) the modulation depth of the NO-Gd ruler is perfectly reproduced with the same setup, therefore, this uncertainty is minimal. The concentration of the rulers was kept quite low to minimize the effects of the background fit on the modulation depth. However, we show now in Fig. R1 the changes in the modulation depth of the NO-Gd ruler in the NOGd channel by varying the power of the pi pulse from that optimized by nutation experiments, and in Fig. R2 the changes in modulation depth by changing the position of the pump pulse from being in the center of the dip to being positioned exactly in the same position in the dip as for the NONO channel.

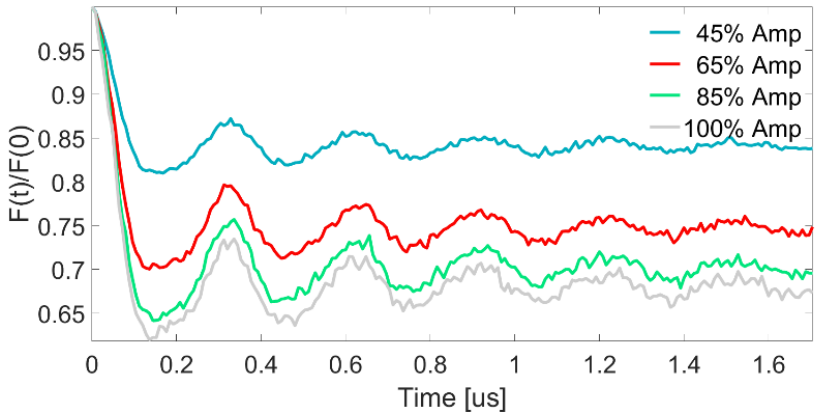

Figure R1: Effect of changing the pump pulse power (AWG amplitude) on the modulation depth in a NOGd DEER setup with a 32 ns pump pulse placed in the center of the dip using the NO-Gd ruler sample. The power optimized via nutation experiments is 65% (26% mod. depth). Interestingly, at higher power, the modulation depth increases (at 85% power it is 30%, and at 100% power it reaches 32%).

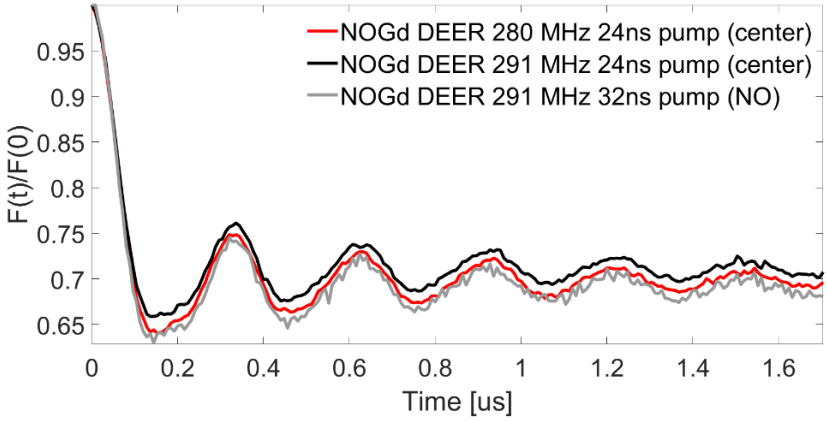

Figure R2: Comparison of different NOGd DEER setups using the NO-Gd ruler sample. Shown in red is the NOGd DEER used in the main text which uses a 24 ns Gaussian pump pulse placed in the center of the resonator dip about 0.4 mT (11 MHz) higher in field than the maximum of the NO spectrum. Show in black is the same setup with the pump pulse placed on the maximum of the NO spectrum (its excitation bandwidth extends over low field side of the spectrum, therefore the mod. depth is a bit smaller). Depicted in gray is the same setup with the pump pulse placed at the same position in the dip as in case of the NONO DEER (about 50 MHz higher in frequency than the center of the dip). The largest deviation between the modulation depths is 2%.

Indeed, the modulation depth of the NOGd channel with the same pump as the NONO channel is slightly smaller than that obtained with the NONO channel. The origin of this effect cannot be a nitroxide radical content <100% in the Gd-NO ruler, therefore effects related to the reduction of the observer echo intensity by the pump might be the reason for the decreased modulation depth detected. This possibility was already addressed as possible source of discrepancies in Shah et al., Inorg. Chem. 2019, citing papers related to the echo reduction effects (Gmeiner et al., PCCP, 2017; Kaminker et al., PCCP, 2012; Yulikov et al., PCCP 2012).

When additional Gd-Gd rulers are present in the sample together with the NO-Gd ruler (in the binary and ternary mixture, the modulation depth decreases reproducibly from 30% to 12.5%, due to the fraction of unmodulated Gd signal which is not dipolarly coupled to the nitroxide moiety. We expected a 6% modulation due to the unmodulated 2xGd-Gd signal intensity in the observer echo, which is lower than the value experimentally obtained. The reason for this discrepancy is unknown, however it could also be related to the observer echo reduction in the presence of the pump pulse, which can affect differently the Gd-Gd rulers and the Gd-NO rulers.

7 Once the modulations depths are quantified and Gaussian contributions to the distances have been fitted it is straightforward to quantify the contributions of the different spin pairs to the DEER signal in question. This is currently only qualitative (e.g., line 140 "with a slightly smaller modulation depth"). The quantified depths can then be compared with the predictions from the respective modulation depths of the pure rulers. I expect to see a table with the different experiments and samples listing the expected and experimentally found modulation depths and contributions of individual rulers expected and found. Finally, you can add the pure ruler DEER signals in the calculated ratios and show that the contributions are similar to experiment and that the analysis does or does not recover the artifact.

The table that you expect to see is the new Table S5 (SI Part B). The ratio of the Gaussian peaks represents the ratio of the respective modulation depths.

Channels and cross-talk

8 I fail to see the benefit this new nomenclature brings over previous descriptions. There may be some point in the choice of these terms but this should be explained comprehensively as currently it only unnecessarily adds to the confusion. Especially assigning the same distance contributions different cross-talk names whether found with a corresponding spin pair present seems arbitrarily expanding the complexity. What is the added value?

Reviewer 1 find that borrowing the nomenclature channel and crosstalk from optics increases the generality, and we agree with his comment. By 'nomenclature' the referee means: the DEER 'channels', the 'crosstalk' signals or the 'name' of the crosstalk signals? We think that using 'crosstalk' signal simplifies the description of the observed peak (it is a signal, not an artifact, and it is due to the spectral overlap which makes it impossible to have clean DEER channels; it should be confused with the '2+1' signal present in DEER if rectangular pulses are used), and it is already used to describe similar effects in microscopy. Added value is clarity, and the compact form X_i simplify the description of the crosstalk signals. We used X_2 and X_3 for the same crosstalk in the presence and absence of a real NOGd signal because it helps the reader to see the differences in the identification and suppression strategies, as explicitly stated in the text.

9 According to figures S4 and S5 you only see the GdGd contribution to GdNO experiment in the equimolar samples and no other crosstalk at all. This means doubling the content of GdGd ruler was done to see the other artifacts at all and is biased from the outset. You should be transparent and explicit about this from the outset when describing the setup and results.

We would like to point out that we always aim to be transparent in our description, however we might have not reached enough clarity. Transparency is a necessary requirement in science.

We chose this ratio for the figures in the main text to highlight the appearance of crosstalk signals. We think that a two-fold excess of the Gd-Gd ruler is still a ratio that can easily occur when studying biological systems. For comparison, we performed the same series of experiments with the three rulers in equimolar concentrations, which can be found in the SI Part B, Table S6 and Fig. S5-S7. We highlighted this more clearly (e.g. first paragraph in section 3.2).

10 You derive conclusions from data you refuse to show. This violates basic research transparency and either the data needs to be added or the statements removed (line 193, 233-234)

This comment is not appropriate. We do not refuse to show data, and we do not violate basic research transparency.

The policy of the journal does not state that 'data not shown' cannot be used. We are very happy to show all data, although especially nutation experiments are never shown in publications. If the referee would like to see other data, we will be happy to provide any information. As discussed in our answer to point 2, we extended Fig. 2 to include more data (see also Table S2, SI Part B).

11 You attribute the GdNO contribution in the NONO experiment to both contributions of Gd to the echo and to the pumped spins. This is based on a 12 dB pump power reduction not altering the modulation depth. How large is the Gd echo at 50K and the chosen refocused echo position? Is it not more likely that the pumping of Gd far off the maximum seems to be invariant to the power levels used in agreement with the data of further experiments (see below)?

We removed this comment, because indeed the minor change observed does not provide enough info.

12 When reducing the pump power in the GdNO experiment this does not seem to alter the GdGd contribution significantly but the GdNO contribution. You state its distance peak intensity increases but contradict this in the next paragraph by stating its modulation depth reduces.

The overall modulation depth reduces, and the relative intensity of the Gd peak increases, this is correct.

You must quantify the contributions (see above) to make quantitative statements.

All modulation depths are now presented in Table S5 (SI Part B).

The statement of “optimized pump power” seems peculiar as the modulation depth reduces with contradicting this more optimum setup. It seems the dependence of the modulation depth on the pump power on Gd away from the maximum is not understood and largely invariant to pump power if not contradicting the predicted trends. The discussion has to reflect this. The power dependence of the spectra in Fig 8 indicate that none of your spins is experiencing the nominal flip angles at 100%.

We agree that the power dependence of the GdGd channel is difficult to interpret. Optimized means ‘by nutation’. Below you find the effects of different pump powers on the GdGd DEER modulation depth (Fig. R3) and on the NONO DEER modulation depth (Fig. R4). In the NONO DEER the modulation depths change as expected, with the maximum being at the optimal pi pump obtained via nutation. In the GdGd channel the behavior is completely different. We cannot explain the deviation observed in the GdGd channel with respect to the expected behavior, but it could be related to the reduction in the observer echo at increasing pump powers (see increasing noise levels in the time traces), and is further complicated by the spectrometer artifact at 3.5 nm. Obviously, the chosen power of the pump pi-pulse optimized by nutation experiments does not provide the maximum modulation depth in GdGd DEER.

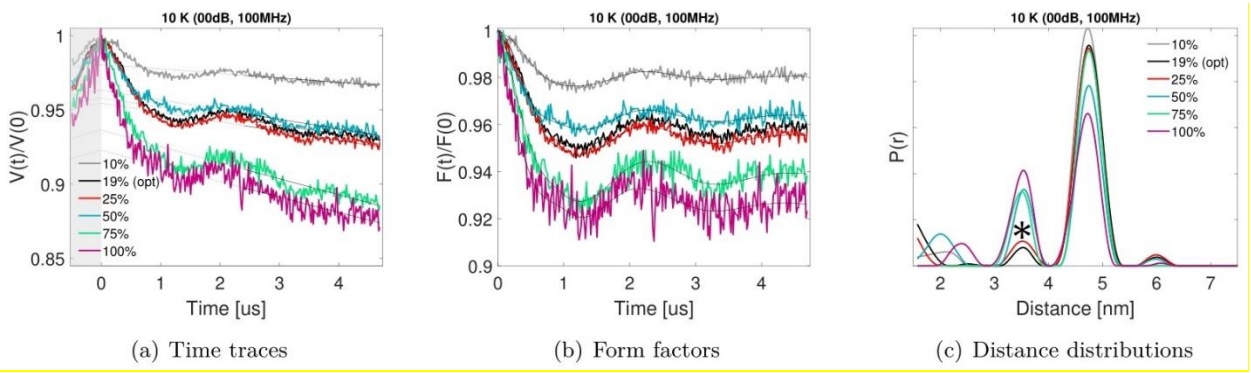

Figure R3: Dependence of the modulation depth on the pump pulse power (AWG amplitude) at 0 dB for a GdGd DEER at 100 MHz separation between the pump and observer frequencies. All pulses were set to 32 ns. All time traces are single scans and just differ by the utilized pump pulse power. The asterisk denotes the spectrometer artifact. The pulse lengths were optimized via nutation experiments. 19% pump pulse amplitude corresponds to a pi-pulse on the spectral maximum of the Gd. The relative intensity of the artifact increases with increasing pump pulses power further complicating the analysis of the modulation depth.

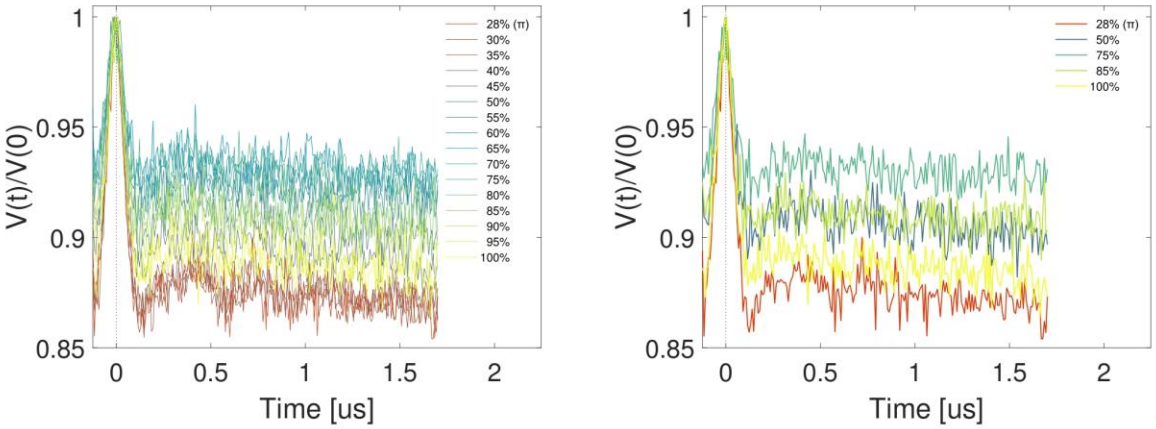

(a) pump pulse amplitude variation (b) pump pulse amplitude variation (selection)

Figure R4: Dependence of the modulation depth on the pump pulse power (AWG amplitude) at 0 dB for a NONO DEER at 100 MHz separation between the pump and observer frequencies. All pulses were set to 64 ns. All time traces are single scans and just differ by the utilized pump pulse power. The pulse lengths were optimized via nutation experiments. 28% pump pulse amplitude corresponds to a pi-pulse on the spectral maximum of the NO.

Spectrometer-specific artifact

13 You should be able to see this artifact in its pure form using a sample of free Gd and NO spin label. How do you know it is an artifact? How do you know it is spectrometer specific? How many other instruments with the same nominal configuration have you tried?

We added a new Fig. S8 (SI Part B) in which DEER time traces were measured on isolated maleimide Gd-DOTA labels in solution to show that this artifact is a sinusoidal oscillation, it is mostly present in the imaginary part of the signal (but clearly it appears also in the real part in some experiments), it is independent of the dipolar frequency, it is not an ESEEM signal, and can be found also in solutions of $MnCl_2$.

GdNO DEER

14 The main potential advantage of NO detected Gd pumped DEER is that 50 K can be used for fast repetition on the nitroxide and diminishing contributions of Gd to the refocused echo as transverse dephasing should be fast. This should definitely be compared experimentally with the other GdNO DEER setup used in here but is not even mentioned. The experiment in Fig 8 done at 50 K will be insightful in first instance.

The sentence "...but experimentally impracticable for samples containing NO and Gd spins due to the prohibitively long shot repetition time of the experiment and the small modulation depths expected." in the conclusion should be adapted in the light of this.

We thank the reviewer for this good idea, indeed we did not try to go higher in temperature. It is tempting to use 50 K because one can use the fast srt due to the fast T_1 of the nitroxide. However, at 50 K the T_1 of the Gd is in the low microsecond time range (see Table S3, SI Part B), therefore the longitudinal relaxation counteracts the inversion induced by the pump pulse within the dipolar evolution time, which is incompatible with DEER. However, we analyzed the relaxation times at different temperatures (see Fig. S3, SI Part B), and found that 30 K was suitable for DEER because the T_1 of the Gd spins is slightly larger than the dipolar evolution time, and we could use an srt of 10 ms (NO observer), detecting DEER traces with a maximal length 2 and 3 microseconds with a good SNR. The swapped NOGd setup allows removing the crosstalk signal, as shown for the X_2 and X_3 cases in new Fig. 9. In the previous version of the paper, we tried only the swapped experiment at 10 K, with an srt of 100 ms, which indeed was impractical due to the too long acquisition time needed. All data are shown in the new Figure 9.

Conclusion

15 The conclusion should not repeat the findings at length but conclude the relevant achievement with respect to the state of the art and the resulting implications and several points of discussion should be moved to the relevant section: -GdGd crosstalk in NONO DEER is likely to be diminished by a negligible Gd refocused echo at 50K and this is why the NO detected GdNO DEER and the Gd transverse dephasing at 50 K need to be given for comparison. -The suggestion to produce new samples lacking certain spins to prove crosstalks is directly opposed to this manuscript's aim. If you make these samples anyways why bother with identifying crosstalks? The GdNO DEER pumping Gd will likely be more cost-effective. -GdGd crosstalk in the GdNO channel can be identified by a minor change in modulation depth upon pump pulse power reduction but if the modulation depth collapses to ∼15% how do I exclude the presence of GdGd crosstalk?

We cut the conclusions. Now that we found a good way to suppress the Gd-Gd crosstalk signal in the NOGd DEER channel, we suggest to produce a new sample only if a signal is present in the NONO DEER channel, which has a distance similar to that obtained in the GdGd channel. If a biological complex mixture of proteins is studied, there might be overlapping real and crosstalk distances, which may complicate the assignment. In case of doubt, before interpreting data erroneously, we believe it is wise to prepare a new sample.

Minor

-"The term orthogonal refers to spin labels that are spectroscopically distinguishable from each other and can be addressed and/or detected independently, e.g. via distinct resonance frequencies, relaxation behavior or transition moments." It would be very helpful to readers if at least one example per concept (frequency, relaxation and nutation filtering) could be given rather than none at all.

The term "orthogonal" is commonly used in literature, we did not introduce it here. We agree that Gd and NO are not perfectly orthogonal, but distinguishable, as shown here. This issue is only a matter of very careful wording and we do not intent to overstretch the meaning of "orthogonal". We changed the title, to account for that.

-In section 1.3 you quantify the spectral widths and relative nutation frequencies but not relaxation differences. You can help the reader by giving longitudinal and transverse magnetization decay constants for both spins at 10 and 50 K to follow this rationale.

We added relaxation data to the manuscript: Table S3-S4 and Fig. S1-S3 (SI PartB).

-Caption figure 4: "Regions in which distances can be theoretically expected". Outline the theory and how this determines where distances can be expected in practice.

Theoretically in that context means 'in principle'. If an overlap exists, one can expect a crosstalk signal. We changed the term 'theoretically possible' to 'possible' (see Fig. 4 and Table S7, SI Part B).

- "Accordingly, we suggest that the dominant signal contribution at 2 nm arising from the NO-NO ruler masks the NO-Gd crosstalk signal." This can easily be checked by synthesizing data from the two pure rulers in the corresponding ratio and analyzing it.

We now provide a relaxation-based rationale for not seeing that artifact when NO signals are present and additionally, we address the excess of NO signal in the echo, which further diminishes the relevance of the crosstalk if NO signals are present.

-Figure S1 You seem to observe some orientation correlation in the GdNO ruler, does the small short-distance spike in the Tikhonov distance distribution correspond to double the frequency of the main peak?

DeerNet does not pick up this small spike (see Fig. 4(a)), therefore we do not consider it in the analysis. Even if there is a minor orientation selection it does not influence the data interpretation, however, we now added this info in the text.

The manuscript has a plethora of general statements that need modification or at least significant context:

-You give 8 nm as upper limit for DEER which is half the current maximum claimed in literature.

We are aware of this publication but we decided to state 8 nm as an upper distance limit for DEER experiments since we believe that 16 nm is not within practically reachable limits considering that it requires a perdeuterated sample in a perdeuterated buffer - i.e. conditions hardly used in structural biology. However, we rephrased the sentence and added this reference (page 1 line 15).

-Your discussion of background correction relies on a homogeneous distribution of spins. This should at least be mentioned.

We added this information (see page 6, line 146). However, due to the low spin concentration, the same results are obtained by 2D or 3D background correction.

-You should clarify the definition of the form factor, when comparing the initial definition by Milov et al. and the more recent use by Jeschke this means different things.

The Form factor is the primary DEER trace divided by the background function and normalized to 1. Added to the first figure legend showing an F(t).

-The multi-spin problem leads to ghost peaks as you rightly state, but it also leads to loss of intensity and resolution at longer distances.

Yes, we added this extra information (see page 2, line 42f).

-Your definition of spectroscopically orthogonal seems ambiguous. As it is impossible to independently address the nitroxide it would fall outside the definition of being orthogonal to the Gd.

This term is used in literature. See comment before on the term ‘orthogonal’. Now in the revised text we make it clear that Gd and NO are non-perfectly orthogonal.

-Spectral overlap between metal ion and nitroxide is common for Gd, Mn, Fe but not for Cu.

This is true, our statement was too general. We removed it from the text.

-"Nitroxides (NO) and GdIII-based spin labels (Gd) are the most commonly used orthogonal spins for DEER experiments on biomolecules." Please provide evidence for this statement. The selective citation practice does not back this up.

We included in the last paragraph of section 1.2 all literature to our knowledge that can be found on NO in conjunction with other spin labels. The amount of publications on NO-Gd-labeled systems strongly supports our hypothesis.

-“For the Gd-Gd crosstalk signals in the NOGd DEER channel, which are the most relevant unwanted signals in the analysis of complex protein mixtures...” There should be evidence provided for this assertion.

This is the output of our comparative analysis. The Gd-Gd crosstalk are the most disturbing and appear in the NOGd DEER channel.

-“Q band currently offers the highest sensitivity to perform the three-channel DEER experiments with samples containing both NO and Gd spin labels on a commercial spectrometer.” There is justification or references needed for this statement.

Justification is provided by discussing the advantages and disadvantages in going to lower and higher frequencies.

~~Orthogonally spin-labeled rulers help~~ Strategies to identify and suppress crosstalk signals ~~and improve~~ in DEER ~~signal fidelity~~experiments

Markus Teucher[1], Mian Qi[2], Ninive Cati[2], Henrik Hintz[2], Adelheid Godt[2], and Enrica Bordignon[1]

[1]Faculty of Chemistry and Biochemistry, Ruhr University Bochum, Universitätsstraße 150, 44801 Bochum, Germany
[2]Faculty of Chemistry and Center for Molecular Materials (CM_2), Bielefeld University, Universitätsstraße 25, 33615 Bielefeld, Germany

Correspondence: Enrica Bordignon (enrica.bordignon@rub.de)

Abstract. ~~DEER spectroscopy applied to orthogonally spin-labeled proteins is a versatile technique which allows simplifying the assignment of distances in complex spin systems and thereby increasing the information content that can be obtained per sample. In fact, orthogonal spin~~ Different types of spin labels can be ~~independently addressed in DEER~~ addressed independently in EPR experiments due to spectroscopically non-overlapping central transitions, distinct relaxation times and/or transition moments~~. Here we focus on molecular rulers orthogonally labeled~~ , hence they are referred to as spectroscopically 'orthogonal'. DEER spectroscopy applied to orthogonally spin-labeled biomolecular complexes allows simplifying the assignment of intra- and inter-molecular distances, thereby increasing the information content per sample. Molecular complexes which are, for example, spin-labeled with nitroxide (NO) and gadolinium (Gd) ~~spins, which~~ labels give access to three distinct DEER ~~'channels', probing~~ "channels", optimized to selectively probe NO-NO, NO-Gd and Gd-Gd distances. ~~It~~ Nevertheless, it has been previously ~~suggested~~ recognized that crosstalk signals between individual DEER channels ~~might~~ can occur, for example, when a Gd-Gd distance appears in a DEER channel optimized to detect NO-Gd distances. This is caused by residual spectral overlap between NO and Gd ~~due to their inevitable spectral overlap. However, a systematic study to address these issues has not yet been carried out~~spins, which therefore, cannot be considered as perfectly 'orthogonal'. Here, we ~~perform a thorough three-channel DEER analysis~~ present a systematic study on mixtures of NO-NO, NO-Gd and Gd-Gd molecular rulers, characterized by distinct, non-overlapping distance distributions~~to study under which conditions crosstalk signals occur and how they can be identified or suppressed to improve signal fidelity. This study will help to improve the assignment of the correct distances~~ , to identify and suppress crosstalk signals in DEER experiments. The strategies presented here will aid the correct assignment of distance peaks in homo- and hetero-complexes of ~~orthogonally spin-labeled proteins~~biomolecules carrying gadolinium and nitroxide spin labels.

1 Introduction

1.1 DEER

Double Electron-Electron Resonance (DEER, also known as PELDOR) is an electron paramagnetic resonance (EPR) pulsed dipolar spectroscopy (PDS) technique introduced by Milov et al. (Milov et al., 1981, 1984) and further developed by Spiess and Jeschke (Martin et al., 1998; Pannier et al., 2000) that probes the r^{-3}-dependent dipolar coupling interaction between adjacent unpaired electron spins. In general, DEER allows the extraction of precise distance information on spin-labeled biomolecules from 1.5 nm to ~~about 8~~6-8 nm, but the upper limit can be extended up to 16 nm~~on spin-labeled proteins in partially deuterated solvents and~~ (Schmidt et al., 2016) for perdeuterated samples. DEER is an established technique in structural biology (Jeschke, 2012, 2018), complementary to X-ray crystallography, NMR spectroscopy and cryo electron microscopy. Perspectively, it is ~~also~~ seen among the most promising methods for in-cell studies (Plitzko et al., 2017).

DEER is usually performed using the dead-time free 4-pulse ~~DEER~~ sequence (Martin et al., 1998; Pannier et al., 2000), a ~~two frequency~~ two-frequency experiment that allows detecting the dipolar modulation of the observer echo induced by changing the position of the pump pulse within the dipolar evolution time. ~~There are two contributions to the time trace :~~ The primary DEER trace contains an inter-molecular background function that needs to be fitted and separated from the desired intra-molecular ~~, desired~~ dipolar signal.

A reliable fit of the background function relies on recording the primary DEER time trace as long as possible, so that the last 2/3 of the trace contains a pure background decay function. This is usually difficult to experimentally achieve for distances $>$ 5-6 nm, especially for samples carrying low concentrations of fast relaxing spins, as it is the case e.g. for spin-labeled membrane proteins. Decreasing the spin concentration alleviates the background problem, because at concentrations $< 10\,\mu M$ the background is an almost flat function, which is easier to be fitted and removed from the trace. Ambiguous background fitting can cause large uncertainties in distance distributions, that can be quantified by data validation approaches ~~in~~ available in most software packages like DeerAnalysis (Jeschke et al., 2006) or LongDistances (Altenbach, 2020).

~~Dividing the~~ Removing the fitted background function from the primary DEER time trace~~by the fitted background function~~ (Ibáñez and Jeschke, 2020) results in the form factor that can be fitted using several approaches, most prominently Tikhonov regularization ~~(Chiang et al., 2005; Jeschke et al., 2006)~~ (Chiang et al., 2005; Jeschke et al., 2006; Edwards and Stoll, 2018) or Gaussian fitting (Brandon et al., 2012; Stein et al., 2015), yielding the distance distribution between intra-molecular dipolarly coupled spins. The recently introduced neural network analysis of DEER data (Worswick et al., 2018) allows direct analysis of primary DEER time traces, providing distance distributions with an uncertainty estimate based on variations in the fits of multiple networks.

1.2 "Orthogonal" spin labeling

In multispin systems carrying the same type of spin label, the assignment of distances within the overall distance distribution can be challenging due to the presence of ghost peaks ~~(von Hagens et al., 2013)~~ (Jeschke et al., 2009; von Hagens et al., 2013), the suppression of long distances (Junk et al., 2011; Ackermann et al., 2017) and the intrinsic difficulties in disentangling

multiple distance contributions, often already when only three spin labels are present in the system (Jeschke et al., 2009; Pribitzer et al., 2017). However, the analysis is simplified for oligomeric systems with a defined symmetry (Valera et al., 2016).

Orthogonal spin labeling ~~(Yulikov, 2015)~~ (introduced by (Lueders et al., 2011; Kaminker et al., 2012; Yulikov et al., 2012)) facilitates the assignment of distances via selectively addressable DEER channels that give access to distance information of specific spin pairs at a time, thereby increasing the information content that can be obtained from a single sample ~~. The term orthogonal refers to spin labels that are spectroscopically distinguishable from each other and can be addressed and/or detected independently, e.g. via distinct resonance frequencies, relaxation behavior or transition moments.~~

~~Two orthogonal~~ (reviewed in (Yulikov, 2015)). In fact, two distinguishable spin labels in a system give access to three DEER channels: two channels probing the interactions ~~between two~~ among the labels of the same type and one channel probing interactions between ~~two different labels~~the two different label types. Depending on the system under study, signals can appear in none, one, two or all three DEER channels. ~~In case of a spectral overlap between the orthogonal labels (which is commonly the case when nitroxides are used in combination with metal ions), crosstalk signals between the DEER channels might appear depending on the degree of orthogonality between the labels and their relative abundance within the sample.This topic has been touched in the literature before (Gmeiner et al., 2017a; Teucher et al., 2019) but was never thoroughly investigated.~~

~~DEER experiments have already been performed~~ The term orthogonal refers to spin labels that are spectroscopically distinguishable from each other and that can be addressed and/or detected independently, e.g. via distinct resonance frequencies, relaxation behavior or transition moments. Despite most spin labels are non-perfectly orthogonal, it was shown that specific inter-spin interactions can be addressed independently, as demonstrated by several publications on a large number of combinations of ~~orthogonal~~ spin labels, e.g. nitroxides in combination with trityl (Shevelev et al., 2015; Joseph et al., 2016; Jassoy et al., 2017), Gd^{III} ~~(Lueders et al., 2011, 2013; Garbuio et al., 2013; Kaminker et al., 2013)~~(Lueders et al., 2011; Kaminker et al., 2012; Yulikov , Fe^{III} (Ezhevskaya et al., 2013; Abdullin et al., 2015; Motion et al., 2016), Cu^{II} ~~(Narr et al., 2002; Meyer et al., 2016)~~ (Narr et al., 2002; Boc or Mn^{II} (Kaminker et al., 2015; Akhmetzyanov et al., 2015; Meyer and Schiemann, 2016). The orthogonal spin labeling approach has also been extended to more than two spin labels (Wu et al., 2017).

In case of a non-negligible spectral overlap of the orthogonal labels, crosstalk signals between the DEER channels might appear depending on the degree of orthogonality between the labels and their relative abundance within the sample. This issue has already been addressed in some studies in literature before (Gmeiner et al., 2017a; Wu et al., 2017; Shah et al., 2019; Teucher et al., 201 , but was not yet systematically investigated.

1.3 ~~Combination~~ The combination of nitroxide and gadolinium^{III} spin labels

Nitroxides (NO) and Gd^{III}-based spin labels (Gd) are ~~the most commonly used orthogonal spins~~ fairly common for DEER experiments on biomolecules. Nitroxides are $S = 1/2$ spin systems with a spectral width in the order of 10 mT at Q band ($\approx$ 35 GHz). Gd^{III}-based spin labels are $S = 7/2$ systems extending over 450 mT at Q band with a sharp central $|-1/2\rangle \rightarrow |+1/2\rangle$ transition whose maximum is usually about 10.4 mT ($\approx$ 291 MHz) higher in magnetic field than the maximum of the NO spectrum. ~~Furthermore, the transition moments and the relaxation behavior of the two spin probes are very distinct allowing for a selective addressability in pulsed EPR experiments. In particular~~The two spins can be selectively addressed

because of their different transition moments (Schweiger and Jeschke, 2001). In fact, a π-pulse for NO corresponds to a $4\,\pi$-pulse for the $|-1/2\rangle \rightarrow |+1/2\rangle$ transition of Gd (Yulikov, 2015), which stands for a 12 dB difference in applied microwave power. ~~Another relevant difference between~~ Additionally, NO and Gd ~~are their~~ have distinct T_1 ~~and T_2~~ relaxation times, ~~which can be used to filter for NO and Gd signals in the DEER observer channel by changing the shot repetition time and the length of the dipolar evolution time, respectively~~therefore, by using short shot repetition times (srt) it is possible to saturate the slow relaxing NO signal at 10 K and enhance the contribution of the Gd signal in the observer echo in DEER (Lueders et al., 2011; Kaminker et al., 2012) .

In this work, we focus on ~~orthogonal~~ three-channel DEER experiments performed at Q band using mixtures of NO and Gd spin labels. These two spin probes give access to three DEER channels, hereafter referred to as: NONO, NOGd and GdGd. We chose three rulers, namely an NO-NO, an NO-Gd and a Gd-Gd ruler with distinct non-overlapping distance distributions to study in a systematic way the signals ~~arising~~ in all detectable DEER channels if one, two or three different rulers are present in the same sample ~~.We identified distance~~ at different stoichiometric ratios. We characterize ruler combinations and DEER channels that are prone to crosstalk signals~~and quantified~~ , quantify their relative strengths ~~thereby providing suggestions on how~~ and provide methods to identify and suppress ~~their~~ the unwanted contributions.

2 Materials and methods

2.1 Samples

~~Here,~~ In this work, we utilized the Gd-Gd ruler Na_2[{Gd^{III}(PyMTA)}-$(EP)_5$E-{Gd^{III}(PyMTA)}] (Qi et al., 2016a), the NO-Gd ruler Na[{Gd^{III}(PyMTA)}-$(EP)_2$-NO•] (Ritsch et al., 2019), and the NO-NO ruler ~~NO~~ON•-$(EP)_2$P-NO• ~~, were used~~ (for structural formulae see Fig. 1). In these compounds two {Gd^{III}(PyMTA)}$^-$ (Qi et al., 2016b) complexes, a {Gd^{III}(PyMTA)}$^-$ complex and a nitroxide, and two nitroxides are held by a rod-like spacer at a distance of 4.7 nm, 2.5 nm, and 2.0 nm, respectively~~, by a rod-like spacer~~. Because of their geometry and the rather high stiffness of the spacer (Jeschke et al., 2010) their interspin distances are well-defined. All rulers are water soluble and can therefore be detected in the same environment as water soluble proteins. The synthesis and characterization of the Gd-Gd and the NO-Gd rulers was published before (Qi et al., 2016a; Ritsch et al., 2019), while the synthesis of the water soluble NO-NO ruler is described in the SI Part A.

The DEER samples were prepared using stock solutions of the rulers in H_2O at concentrations of 50 - 100 µM. To each sample 50% v/v deuterated glycerol was added as cryoprotectant yielding the final spin concentrations given in Table S1 (SI Part B). 40 µl of each sample were inserted into 3 mm outer diameter quartz tubes and shock frozen in liquid nitrogen.

2.2 Instrumentation

2.2.1 ~~Spectrometer~~Spectrometers

Continous wave (cw) EPR experiments for NO spin counting were performed at X band using a MiniScope MS 5000 spectrometer (Magnettech by Freiberg Instruments). All pulsed EPR experiments were performed using a Bruker Biospin Q-band

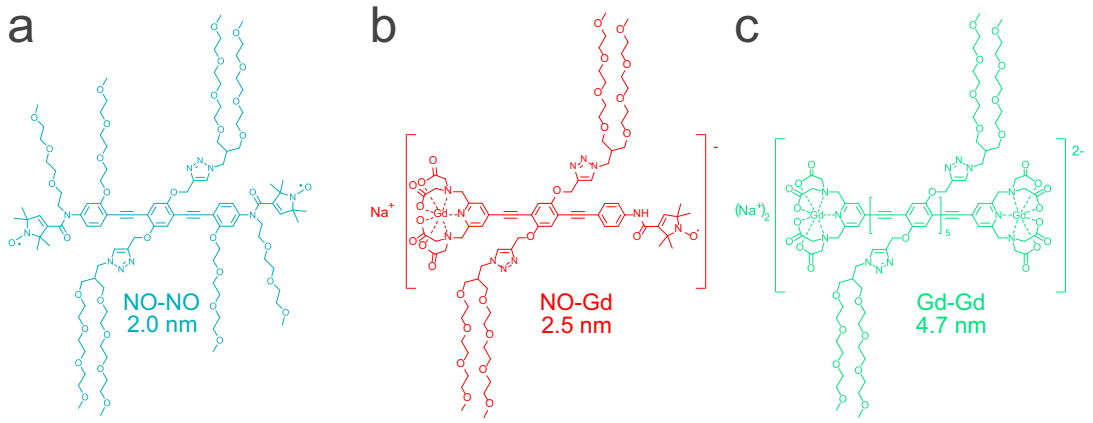

Figure 1. Structural formulae of the NO-NO, NO-Gd and Gd-Gd rulers. Indicated are the experimentally detected mean distances between the paramagnetic centers.

Elexsys E580 spectrometer equipped with a 150 W TWT amplifier from Applied Systems Engineering and a Bruker SpinJet-AWG (±400 MHz bandwidth, 1.6 GSa/s sampling rate, 14 bit amplitude resolution) in combination with a home-made Q-band resonator for 3 mm sample tubes (Tschaggelar et al., 2009; Polyhach et al., 2012).

2.2.2 ~~Pulse parameters~~Transient nutation experiments

~~All pulse~~ Nutation experiments were performed using ~~monochromatic pulses with a Gaussian amplitude modulation function, predefined as pulse shape~~the sequence (nutation pulse)-(1000 ~~1 in Bruker Xepr 2.6b.119. In Xepr, the pulse length t_p of a Gaussian pulse is defined as its timebase (truncation at 2.2% of its maximum amplitude~~ns)-(π/2)~~which is related to its full width at half maximum (FWHM)by $t_p = 2\sqrt{2ln2} \cdot FWHM \approx 2.3548 \cdot FWHM$ (Teucher and Bordignon, 2018).~~400 ns)-(π)-(400 ns)-(echo) with 16 ns for the π/2-pulse and 32 ns for the π-pulse. The nutation pulse length was incremented starting from 0 in 2 ns steps and the position of the detection pulses and of the acquisition trigger was displaced using the same increment. For the data shown in Fig. 2, the frequency was placed in the center of the resonator dip and the amplitudes of all pulses were changed from 100 to 10% keeping the main attenuator at 0, 6, or 12 dB. The intensity of the echo (single point detection on the maximum) was recorded versus the nutation pulse length and the position of the first minimum of the nutation transient was taken as the π-pulse length (Fig. 2, first three columns). The rightmost column in Fig. 2 shows the correlation between the amplitude of the AWG-pulses (expressed in %) and the π-pulse length for the different main attenuator settings (in dB). All experiments were performed using the NO-Gd ruler, placing the field either at the maximum of the Gd signal ($|-1/2\rangle \rightarrow |+1/2\rangle$ transition) or at the maximum of the NO (Fig. 2(a) and (b)). The nutation transients show only minor variations in the AWG amplitude range 80-100%, however, from 80 to 10% the continuous increase of the pulse length for a π-pulse could be followed (Fig. 2). The analysis of the data shows that at 12 dB attenuation, a 30 ns π pulse can be obtained at 80% pulse amplitude, while at 6 dB approximately 40%, and at 0 dB about 20% pulse amplitude are required to obtain 28 and 27 ns π pulses, respectively. This demonstrates a linear power scaling for the main attenuator and the AWG, as halving B_1 (6 dB attenuation in power) requires

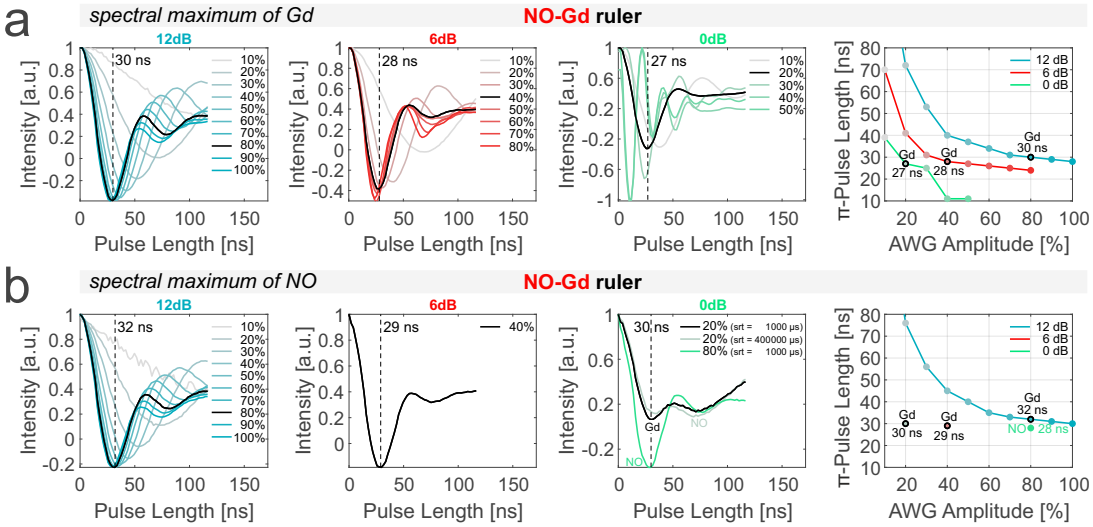

Figure 2. Power dependence of NO and Gd π-pulses. Transient nutation experiments were performed at different spectral positions of the NO-Gd ruler at 10 K. Data were recorded at 12, 6 and 0 dB attenuation (columns 1 to 3), varying the AWG amplitude. The fourth column shows the correlation of the extracted π-pulse lengths (first minimum of the nutation transient) and the AWG pulse amplitude (in %) for the different main attenuator settings (in dB). All extracted π-pulse lengths are given in Table S2 (SI Part B). The transients shown in (a) were recorded on the spectral maximum of the Gd and in (b) on the maximum of the NO-spectrum which is 10.4 mT lower in magnetic field than the maximum of the Gd for the utilized sample (see Fig. 3) using a shot repetition time (srt) of 1000 µs (if not stated differently). (a) In our setup, 12 dB attenuation and 80% AWG amplitude correspond to a 30 ns Gaussian π-pulse. Doubling the power (6 dB) is shown to require halving the AWG amplitude (highlighted in black for a ≈ 30 ns π-pulse). (b) An srt of 1000 µs makes the nutation experiments more sensitive to Gd at 10 K (see relaxation data given in Fig. S1 to S3 and Table S3 to S4, SI Part B). At 0 dB main attenuation and 20% AWG amplitude the nutation of the NO becomes also visible (black). Prolonging the srt to 400,000 µs at 20% amplitude slightly increases the amplitude of the NO nutation with respect to the nutation of Gd (gray). A pulse amplitude of 80% gives also 30 ns π-pulse length (green), which corresponds to a π-pulse on the NO spins.

a decrease of the AWG amplitude from 80% to 40% and a decrease by a factor of 4 (corresponding to 12 dB) correlates with a change in the AWG amplitude from 80% to 20%.

The same trend could be detected at the maximum position of the NO spectrum, using a shot repetition time (srt) of 1000 µs, which saturates the NO signal and thereby enhances the Gd signal (Fig. 2(b)). Therefore, we can conclude that we sample mostly the Gd $|-1/2\rangle \rightarrow |+1/2\rangle$ transition even at 10.4 mT lower in field with respect to the maximum of the Gd spectrum. To address the complications arising from the overlap of the NO and Gd signals (see Fig. 3), we performed nutation experiments at 0 dB and 20% AWG amplitude on the maximum of the NO spectrum using different srt values (Fig. 2(b), third column). Using a fast srt of 1000 µs, two minima of nearly equal intensity are detected in contrast to the single minimum for the nutation performed on the maximum of the Gd using the same parameters. These minima are created by the superposition of the nutations of the Gd (first minimum at 30 ns) and the NO spins (second minimum). Because of the slow T_1-relaxation of the NO

at 10 K, performing the same experiment at srt 400,000 µs increases the contribution of the nitroxide-related minimum. When the AWG amplitude is set to 80% (which corresponds to a 12 dB increase in power with respect to the 20% amplitude), we detected a first minimum at 30 ns, which is attributable to a π-pulse for the NO spins. In fact, at this power the π-pulse for the Gd spins should be ≈ 10 ns (see Fig. 2(a)). Therefore, changing the microwave power by 12 dB (e.g. from 80 to 20% AWG amplitude) allows to selectively address either Gd or NO spins. Overall, the nutation experiments allow a precise determination of the optimal length of the π-pulses for NO and Gd in all DEER setups.

2.2.3 DEER setup

DEER experiments were performed using the dead-time free 4-pulse ~~DEER~~ sequence $(\pi/2)_{obs} - (d_1) - (\pi)_{obs} - (d_1+T) - (\pi)_{pump} - (d_2-T) - (\pi)_{obs} - (d_2) -$ (echo) (Martin et al., 1998; Pannier et al., 2000) with 16-step phase cycling (Tait and Stoll, 2016) using (0)-(π) for $(\pi/2)_{obs}$ and $(\pi)_{obs}$, and (0)-(π/2)-(π)-(3π/2) for $(\pi)_{pump}$. ~~Gaussian~~ All pulse experiments were performed using monochromatic pulses with a Gaussian amplitude modulation function, predefined as pulse shape 1 in Bruker Xepr 2.6b.119. In Xepr, the pulse length t_p of a Gaussian pulse is defined as its time base (truncation at 2.2% of its maximum amplitude) which is related to its full width at half maximum (FWHM) by $t_p = 2\sqrt{2ln2} \cdot \text{FWHM} \approx 2.3548 \cdot \text{FWHM}$ (Teucher and Bordignon, 2018) . Gaussian π/2- and π-pulses at the observer frequency were created by varying the pulse amplitude at a fixed pulse length to maintain a uniform excitation bandwidth for the refocused echo (Teucher and Bordignon, 2018). The length of the Gaussian pulses was optimized individually for each experiment via transient nutation experiments~~for each spin type~~ , as shown in Fig. 2. ~~The~~

In all DEER experiments, the main frequency of the microwave bridge was set to the observer position with the AWG synthesizing the frequency offset required for the pump pulse. More details about the ~~DEER setups for the orthogonal spin probes~~ utilized three-channel DEER setups are given in Fig. 3. The evaluation of the DEER data was performed with DeerAnalysis2019 using the Gaussian fitting routine ~~of DeerAnalysis2019 (Jeschke et al., 2006)~~assuming a homogeneous 3D background function and the neural network analysis (DeerNet) (Jeschke et al., 2006; Worswick et al., 2018) to obtain an error estimation. Gaussian fitting was chosen over Tikhonov regularization since it simplifies data evaluation for distributions with well-defined ~~narrow distance distributions as it is the case for the rulers. In particular, it~~ distance peaks, allows simultaneous fitting of components with very different distribution widths ~~as required for the utilized samples. A side-by-side comparison of both methods is presented~~ and enables quantification of the relative contributions of the distance peaks, which is optimal for the analysis performed. However, a comparison of Gaussian and Tikhonov analysis can be found in Fig. ~~S1~~ S4 (SI Part B).

~~NO and Gd nutation experiments. Transient nutation experiments performed at 10 K with different shot repetition times (srt) and pulse amplitudes within the spectral overlap of NO and Gd (at the maximum of the NO signal). Based on the different longitudinal relaxation times of the two spin probes, srt filtering allows independent addressability. Adjusting the pulse amplitudes allows matching the π-pulse lengths of NO and Gd. At an srt of 300 ms the predominant nutation signal contribution arises from the NO which has in the center of the dip at 100% AWG amplitude a 24 ns (10.2 ns FWHM) Gaussian π-pulse length. Decreasing the srt from 300 ms to 1 ms allows filtering for Gd, which matches the 24 ns π-pulse length at 22% AWG~~

~~amplitude. This difference in AWG amplitude corresponds to a 12 dB difference in power between NO and Gd (Yulikov, 2015) based on their distinct transition moments.~~

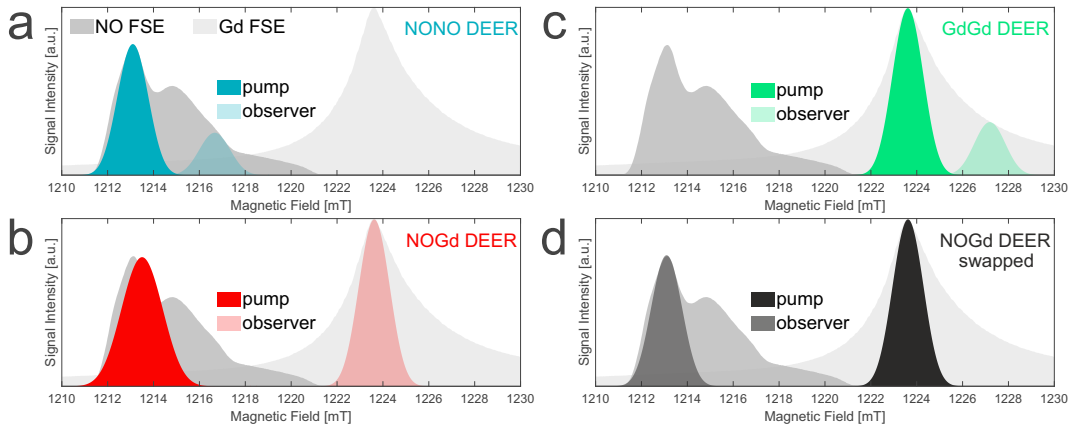

Figure 3. ~~Three-channel~~ Three-channel DEER setups. NO and Gd field-swept echo (FSE) spectra are shown as shaded gray areas~~with overlaid~~ . Gaussian ~~pump and observer~~ π-pulse excitation profiles are shown at the respective pump and observer positions, simulated with EasySpin 5.2.2 (Stoll and Schweiger, 2006) using the provided functions 'pulse' and 'exciteprofile'. The excitation profiles represent ideal Gaussian π-pulses, without taking into account the spectral shape, the non-linearity of the signal response, the resonator profile and the Q factor. Nevertheless, we found that such profiles are sufficient to the correctly choose the pulse lengths and the frequency separation between the pump and observer to experimentally minimize the pulse overlap, and consequently the '2+1' signal at the end of DEER traces (Teucher and Bordignon, 2018). In ~~all~~ setups (a-c), Gaussian observer pulses of 32 ns time base length (13.6 ns FWHM) for π/2 and π (Teucher and Bordignon, 2018) were used in combination with a shot repetition time (srt) of 1000 µs. (a) NONO DEER: 32 ns Gaussian pump ~~on~~ at the spectral maximum of NO; observer pulses 100 MHz lower in frequency; pump/observer placed symmetrical in resonator profile; performed at 50 K. (b) NOGd DEER: 32 ns Gaussian observer pulse at the spectral maximum of Gd; Gaussian pump pulse of 24 ns (10.2 ns FWHM) ~~Gaussian pump~~ placed in the center of the resonator profile ~~; pump position 0.4 mT higher~~ (minimum possible pulse length in ~~field than the spectral maximum of NO with observer~~ our setup) 280 MHz ~~lower~~ higher in frequency ~~on spectral maximum of Gd~~than the observer; performed at 10 K. (c) GdGd DEER: as in (a), except for the pump pulse placed on the maximum of the Gd spectrum; performed at 10 K. (d) Swapped NOGd DEER setup: 32 ns Gaussian observer pulses at the spectral maximum of NO; 32 ns Gaussian pump pulse 291 MHz lower in frequency than the observer; performed at 30 K with an srt of 10,000 µs. Observer placed +50 MHz off-center in the resonator profile.

2.2.4 Relaxation measurements

185 T_1 and T_m relaxation measurements were performed at different temperatures on all samples at different spectral positions corresponding to the pump/observer positions of the DEER setups introduced in Fig. 3. The relaxation data are shown in Figs. S1-S3 and Tables S3-S4 (SI Part B).

T_1 was measured using the inversion recovery sequence (π)-(T)-(π/2)-(180 ns)-(π)-(180 ns)-(echo) with a 32 ns Gaussian inversion π-pulse separated by a variable time T from the 16-32 ns Gaussian echo sequence. The signal was recorded by

integrating over the FWHM of the echo (= 32 ns) and plotting the echo intensity versus T. The initial time T was set to 800 ns and incremented in N·ΔT steps. The T_1 values were extracted in MATLAB assuming a Bloch model for relaxation. The fully recovered magnetization was normalized to one and T_1 was extracted as the time where the echo intensity reaches a value of 0.26 according to:

$$I(t) = 1\left(1 - 2\,e^{-\frac{T}{T_1}}\right) \tag{1}$$

with $T = T_1$

$$I(t) = 1\left(1 - \frac{2}{e}\right) \approx 0.26 \tag{2}$$

Based on the small variations in the values obtained when a sample is remeasured we conservatively estimate an error of 5%.

T_m was measured using the echo decay sequence (π/2)-(T)-(π)-(T)-(echo) with 16-32 ns Gaussian pulses separated by a variable time T. The signal was acquired by integrating over the FWHM of the echo (= 32 ns) with an initial interpulse delay T of 180 ns which was incremented in N·ΔT steps. The echo intensity was plotted versus the interpulse delay T. As commonly reported in literature, the T_m values were extracted using MATLAB from the echo decay curves as the time T at which the echo intensity is decayed to 10% of its original value. There is a small variation in the obtained values when a sample is remeasured and we estimate an error of 10%.

3 Experimental results and discussion

3.1 Isolated rulers

The DEER characterization of the three individual rulers is shown in Fig. 4. Since ~~both~~ the NO-NO and the Gd-Gd rulers contain only one type of label, we ~~could probe per sample~~ probed only one DEER channel per sample, namely the NONO or GdGd channel, respectively~~, whereas the orthogonally labeled~~ . For the NO-Gd ruler ~~gives access to~~ we probed all three DEER channels. ~~Notably, the obtained dipolar frequencies~~The dipolar frequencies, distance distributions and modulation depths ~~of the isolated ruler samples with their corresponding distance distributions~~ obtained on the isolated rulers are characteristic sample- and setup-dependent parameters which will be used in the following to identify and quantify crosstalk signals in the ruler mixtures. An overview of all DEER data and the quantification of the fractions of each distance peak in the overall distribution is given in Table S5 (SI Part B).

The NONO DEER time trace (blue) detected on the NO-NO ruler in Fig. 4(a) shows a dipolar frequency ~~characterized by~~ with a 35% modulation depth, corresponding to a well-defined 2 nm distance. The GdGd DEER time trace (green) detected on the Gd-Gd ruler shows a dipolar frequency with a modulation depth of ≈ 3%, corresponding to a monomodal distance distribution centered at 4.7 nm (see Fig. 4(b)). The uncertainties in the distance distributions for both rulers are are negligible, as shown by the neural network analysis presented in Fig. 4(b,c). The Tikhonov analysis is shown in Fig. S4 (SI Part B).

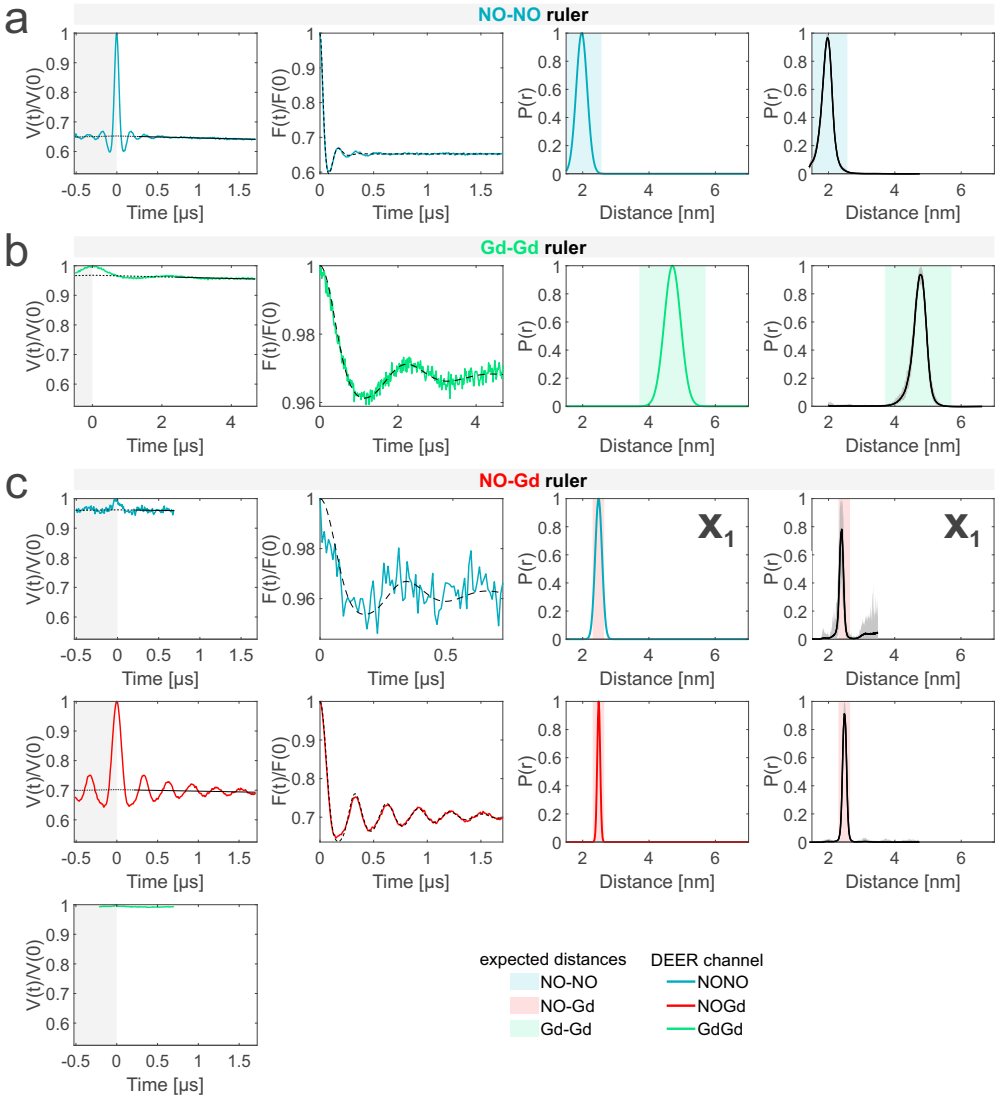

Figure 4. Characterization of the isolated rulers. The DEER setups are introduced in Fig. 3. ~~Left~~First column, primary data with background fit (gray areas are excluded from data evaluation); ~~middle~~second column, form factors (obtained by dividing the primary data by the background function) with ~~Gaussian~~ fit from Gaussian fitting routine; ~~right~~third column, obtained distance distributions; fourth column, DeerNet analysis (Generic network) to provide an error estimation. A Tikhonov analysis of the data is shown in Fig. ~~S1~~ S4 (SI Part B). An overview over all DEER data is given in Table S5 (SI Part B). The time traces, form factors and distance distributions recorded with the NONO DEER channel are colored in blue, those recorded with the GdGd channel are colored in green, and those recorded with the NOGd channel are colored in red. Regions in which distances can be ~~theoretically~~ expected based on the rulers present in the specific sample are represented as shaded blue, green and red areas in the distance distributions. "$\mathbf{X}_1$" is ~~an~~ a NO-Gd crosstalk in the NONO DEER channel.

The time traces obtained on the NO-Gd ruler with the three DEER channels are shown in Fig. 4(c). The NOGd DEER time trace (red) shows a defined dipolar frequency ~~which is characterized by a~~ (30% modulation depth~~and correlates~~) correlated with a 2.5 nm distance. The distance obtained via neural network analysis is consistent and shows negligible uncertainties. However, Tikhonov analysis extracted an additional peak of low intensity centered at 2 nm, which could be consistent with minor orientation selection effects (Fig. S4 (SI Part B)). Unexpectedly, the NONO DEER channel (blue) also contains a dipolar signal with 4% modulation depth whose distance distribution coincides with the one obtained in the NOGd DEER channel. ~~In contrast, the GdGd channel (green) contains a mere background function. The absence of a dipolar modulation in the GdGd DEER channel proves that the NO-Gd ruler is monomeric in solution. Therefore, we can conclude that the signal detected in the NONO DEER channel is a crosstalk signal. This crosstalk signal originates from a residual excitation of the Gd spectrum overlapping with the nitroxide spectrum by the~~ This is a DEER channel crosstalk signal, caused by the unintended excitation of spectrally overlapping Gd spins via the pump and/or observer pulses~~in the NONO DEER sequence.This~~ . Due to the fast phase memory time of the nitroxide spins in the NO-Gd ruler at 50 K (see Fig. S2 and Table S4, SI Part B), only a noisy 1 µs trace could be detected, and as a consequence, the neural network analysis provides larger uncertainties in the main distance peak. Such a crosstalk signal is significant, because its ≈4% modulation depth is in the order of 10% of the maximally achievable modulation depth for the spin-labeled NO-NO ruler (see Fig. 4(a)). We classify this signal as a NO-Gd crosstalk in the NONO DEER channel and designate it as $\mathbf{X}_1$. The GdGd channel (green) shows no dipolar modulation, confirming that the NO-Gd ruler is monomeric in solution and that the signal detected in the NONO DEER channel is indeed a crosstalk signal between DEER channels.

3.2 Ruler mixtures

In this section we investigate the appearance of crosstalk signals between the DEER channels in samples containing ~~pairwise mixtures of the~~ mixtures of two or three rulers. ~~The data are presented in~~ We chose to analyze two different molar ratios to address the effect of relative spin concentrations on the strength of the crosstalk signals. The data with a 2-fold excess of the Gd-Gd rulers with respect to the others is presented in the main text, while we show a full data set of the rulers in equimolar mixtures in the SI (Table S6 and Figs. S5-S7, SI Part B). The reproducibility of the data presented are shown with independent repetitions performed on the isolated rulers in Fig. ~~5.~~S5 and on the mixtures of two rulers in Fig. S6.

The three DEER experiments performed on the mixture of the NO-NO ruler with the NO-Gd ruler in a 1:1 molar ratio are shown in Fig. 5~~(a)~~. The NONO DEER channel contains the expected distance distribution of the isolated NO-NO ruler characterized in Fig. 4(a)~~with a slightly smaller modulation depth~~. The NOGd channel reproduces the signal obtained on the isolated NO-Gd ruler previously shown in Fig. 4(b). The GdGd channel shows no dipolar modulation, in line with the absence of Gd-Gd rulers in this sample.

The NO-Gd crosstalk signal previously detected in the NONO channel ($\mathbf{X}_1$) ~~detected~~ for the isolated NO-Gd ruler in the mixture of the NO-NO with the NO-Gd rulers in Fig. 4(c) ~~would be theoretically expected at 2.5 nm. Interestingly, this signal~~ is not experimentally resolved ~~in the mixture of NO-NO ruler with~~ (see Fig. 5). If we consider that the NO spins of the NO-Gd ruler ~~. As addressed before, this crosstalk signal is caused by a residual excitation of Gd spins via the NO-optimized pump~~

and/or observer pulses. When considering that the pump pulseexcites the Gd spins, and the observer excites the are observed and the Gd spins are partially excited by the pump pulse, we suggest that the absence of this crosstalk signal is due to the fact that the NO spins of the NO-Gd ruler , one needs to take into account that in have a shorter phase memory time T_m than those in the NO-NO ruler at 50 K ($T_m \approx 2\,\mu s$ versus 4.6 µs, see Fig. S2 and Table S4, SI Part B), which strongly decreases their contribution in the observer echo for the detected 2 µs time trace. Additionally, in this sample, only 1/3 of the NO observer signal in the NONO channel originates from the NO-Gd ruler, which would will further decrease the modulation depth of the crosstalk signal from the 4% detected on the isolated with respect to the case in which only the NO-Gd ruler is present (see Fig. 4(c)), to 1% for this sample, which is hardly detectable. When considering that the NO-optimized observer pulse excites the residual Gd spins of the NO-Gd ruler , one has to consider that the overall observer echohas a predominant NO contribution and therefore an even lower modulation depth is expected. If we consider that the Gd spins are partially observed and the NO spins are pumped, the presence of the NO-NO ruler reduces the relative contribution of the Gd spins in the observer echo, thereby decreasing the modulation depth of the crosstalk signal. Accordingly, we suggest that the in this mixture the NO-Gd crosstalk signal is negligible and only the dominant signal contribution at 2 nm arising from the NO-NO ruler masks the NO-Gd crosstalk signalis detectable.

The analysis of the sample containing the NO-NO ruler and the Gd-Gd ruler in a 1:2 or 1:1 molar ratio is presented in Fig. 56 and Fig. S6(b) .(SI Part B), respectively. No differences could be observed when different ratios were used. Both the NONO and the GdGd channels reproduce nicely the DEER signals obtained on from the isolated NO-NO and Gd-Gd rulers. As there is no NO-Gd ruler present in the sample, no signal would be expected in the respective DEER channel. Indeed, no NO-Gd distance was detected but, instead, However, a dipolar frequency was detected with a 4% modulation depth, which is attributed to a Gd-Gd crosstalk signal was visible in the NOGd channel (defined as $\mathbf{X}_2$). Apart from that, the NOGd channel contains a secondary , as shown by the fit performed with a single Gaussian centered at the same mean distance as that of the isolated Gd-Gd ruler (see Fig. 6, solid line). The neural network analysis revealed a second distance peak centered at 3.5 nm distance which originates from a spectrometer-specific oscillatory signal of constant amplitude present in the time domain trace which is discussed in more detail in section 3.3. The modulation amplitude of this spectrometer artifact adds up to the modulation depth of (highlighted with an asterisk), which can also be found when fitting the data with two Gaussian peaks, which improves the root mean square deviation between fit and data (Fig. 6, broken line). To understand the origin of the Gd-Gd crosstalk signal . The actual crosstalk signal has a modulation depth ofabout 3% which is (as in the case of the NO-Gd crosstalk in the NONO channel, defined as $\mathbf{X}_1$) in peak at 3.5 nm, a series of DEER experiments using a stock solution of Gd-maleimide DOTA was performed. It was found that the 3.5 nm peak arises from a sinusoidal signal with a frequency of ≈ 1 MHz which is independent on the chosen srt. This signal has no dipolar origin, we can exclude that it is an ESEEM effect, and it appears also in $MnCl_2$ solutions. We could remove it only by decreasing the power of the order of 10% of the maximally expected modulation depth of 30% in this channel (see pump pulse to zero (more information in Fig. 4(c)) and therefore non-negligibleS8, SI Part B). Therefore, we assign the 3.5 nm peak to an artifact in our setup. The strength of this artifact varies in different measurements and it is mostly visible when traces with small modulation depths and high signal-to-noise are detected.

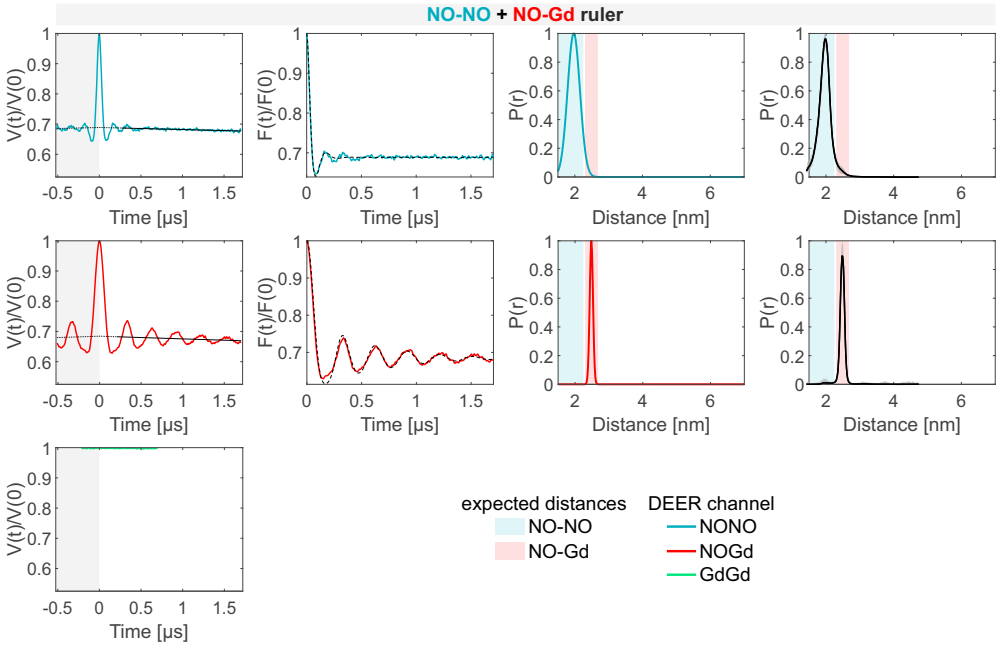

Figure 5. ~~Pairwise mixtures of rulers. The DEER setups are introduced in Fig. 3. Left, primary data with background fit (gray areas are excluded from data evaluation); middle, form factors with Gaussian fit; right, obtained distance distributions. Color coding as in Fig. 4. (a)~~ Sample containing the NO-NO and the NO-Gd rulers mixed in a 1:1 molar ratio. ~~(b) Sample containing~~ The legend is the ~~NO-NO and the Gd-Gd rulers mixed~~ same as in ~~a 1:2 ratio~~Fig.~~The NOGd DEER channel contains a Gd-Gd crosstalk signal~~ $\mathbf{X}_2$4. ~~The distance indicated with an asterisk originates from a spectrometer-specific artifact signal. (c) Mixture of the NO-Gd ruler with the Gd-Gd ruler in a 1:2 ratio. NO-Gd~~ No crosstalk ~~signal~~ signals are detected in ~~the NONO channel ($\mathbf{X}_1$) and Gd-Gd crosstalk signal in the NOGd channel in presence of an NO-Gd signal ($\mathbf{X}_3$)~~this sample.

The results of the experiments with the 1:2 mixture of the NO-Gd ruler with the Gd-Gd ruler are presented in Fig. ~~5(c)~~7. The NONO DEER channel of this sample shows the NO-Gd crosstalk signal in the NONO DEER channel ($\mathbf{X}_1$) as reported for the isolated NO-Gd ruler in Fig. 4(c). ~~The identification~~ Likewise, just a short time trace could be recorded due to the fast phase memory time of the NO spins in the NO-Gd ruler (see Fig. S2 and Table S4, SI Part B). The presence of this crosstalk signal ~~is facilitated by~~ corroborates our interpretation that it can be detected only in the absence of ~~a real NO-NO distance~~extra NO spins in the sample. The GdGd channel ~~, due to the absence of any spectral overlap~~ in our DEER setup ~~, is intrinsically artifact-free~~ (pump at the maximum of the spectrum and observer at a higher field, see Fig. 3(c)), is intrinsically crosstalk-free and shows the expected pure Gd-Gd distance. In contrast, the NOGd channel contains, besides the expected NO-Gd distance, a Gd-Gd crosstalk signal defined as $\mathbf{X}_3$ which is ~~not~~ fully resolved in the ~~1.7~~4.7 µs time trace presented in Fig. ~~5(c). However, it is clearly visible in a longer time trace presented in section 3.3.~~$\mathbf{X}_2$ ~~in~~ 7.

However, this crosstalk signal could not be identified in the 1:1 mixture, indicating that the relative concentration of the Gd-Gd ruler modulates the intensity of such unwanted signal in the NOGd channel (see Fig. 7 versus Fig. ~~5(b)and~~ $\mathbf{X}_3$ ~~in~~ S6(c),

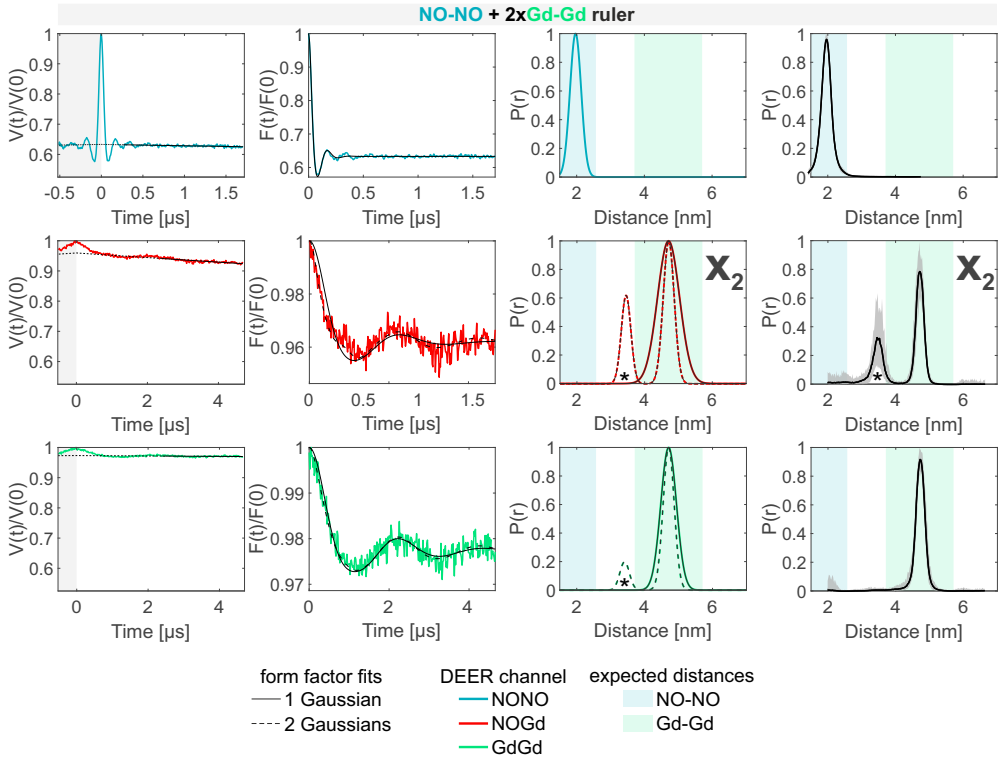

Figure 6. Sample containing the NO-NO and the Gd-Gd rulers mixed in a 1:2 molar ratio. The legend is the same as in Fig. 4. The form factors in the NOGd and in the GdGd channel were fitted using both a single Gaussian (solid line) and two Gaussians (broken line) to highlight the appearance of a spectrometer-specific artifact signal corresponding to a 3.5 nm distance (highlighted with an asterisk, see Fig. S8, SI Part B). The NOGd DEER channel contains a Gd-Gd crosstalk signal in absence of a NO-Gd distance designated as $\mathbf{X}_2$. A comparison on how different neural networks fit this crosstalk signal is shown in Fig. S9(a) (SI Part B).

SI Part B). The crosstalk signals identified in the NOGd DEER channel in Fig. ~~5(c)~~ 6 and Fig. 7 are both Gd-Gd crosstalk signals in the NOGd channel, however, we decided to keep a distinction in the names based on the absence/presence of a "real" NO-Gd distance which will have an influence on the identification and suppression procedure discussed below.

The DEER data obtained on the sample containing the NO-NO, NO-Gd and Gd-Gd rulers in a 1:1:2 ratio are presented in Fig. ~~6~~8. Essentially, these data can be seen as a superposition of the data detected on the pairwise mixtures of rulers. The NONO DEER channel shows the distance distribution of the NO-NO ruler but lacks the $\mathbf{X}_1$ crosstalk signal ~~because it is masked by the intensity of the NO-NO DEER signal~~due to the presence of additional NO signals. Besides the expected NO-Gd ruler distance, the NOGd channel shows the Gd-Gd crosstalk signal $\mathbf{X}_3$ as in Fig. ~~5(c)~~7, which is clearly visible in the asymmetry of the time trace due to the underlying low frequency characteristic of the Gd-Gd ~~signal~~dipolar function. Finally, the GdGd DEER channel resolves the Gd-Gd distance free of crosstalk signals.

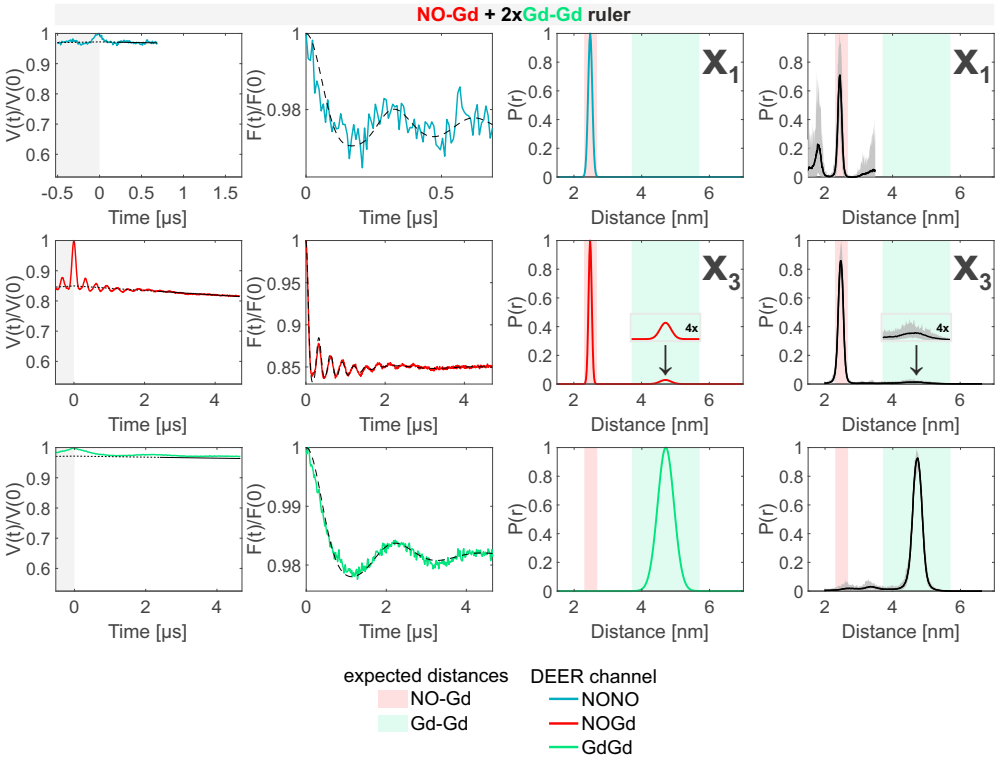

Figure 7. Sample containing the NO-Gd and the Gd-Gd rulers mixed in a 1:2 molar ratio. The legend is the same as in Fig. 4. The NONO DEER channel contains a NO-Gd crosstalk signal ($\mathbf{X}_1$) and the NOGd channel contains a Gd-Gd crosstalk signal in presence of a NO-Gd distance designated as $\mathbf{X}_3$. A comparison on how different neural networks fit this crosstalk signal is shown in Fig. S9(b) (SI Part B).

In conclusion, we identified three non-negligible crosstalk signals in the NONO and NOGd DEER channels and we showed that the GdGd DEER setup with the observer frequency placed on the maximum of the Gd signal and the pump frequency at the high field edge of the Gd spectrum (see Fig. 3(c)) is intrinsically crosstalk-free in all experimental conditions tested.

3.3 DEER channel crosstalk identification and suppression

The DEER ~~channel~~ crosstalk signals discussed in this work are named as follows: $\mathbf{X}_1$ ~~is an~~ is a NO-Gd crosstalk signal in the NONO channel, while $\mathbf{X}_2$ and $\mathbf{X}_3$ are both Gd-Gd crosstalk signals in the NOGd channel but either in the absence or presence of a "real" NO-Gd signal, respectively. An overview of all crosstalk signals that ~~can be theoretically expected versus those that were experimentally detected using our samples and experimental setups~~ are possible to occur based on the spectral overlap between NO and Gd at the pump and/or observer positions and those experimentally detected with our sample/setup combination is presented in Table ~~S2~~ S7 (SI Part B).

The origin of ~~all crosstalk signals reported in this work is the spectral overlap between NO and Gd illustrated in Fig. 3(b), which does not allow a completely independent addressability.~~

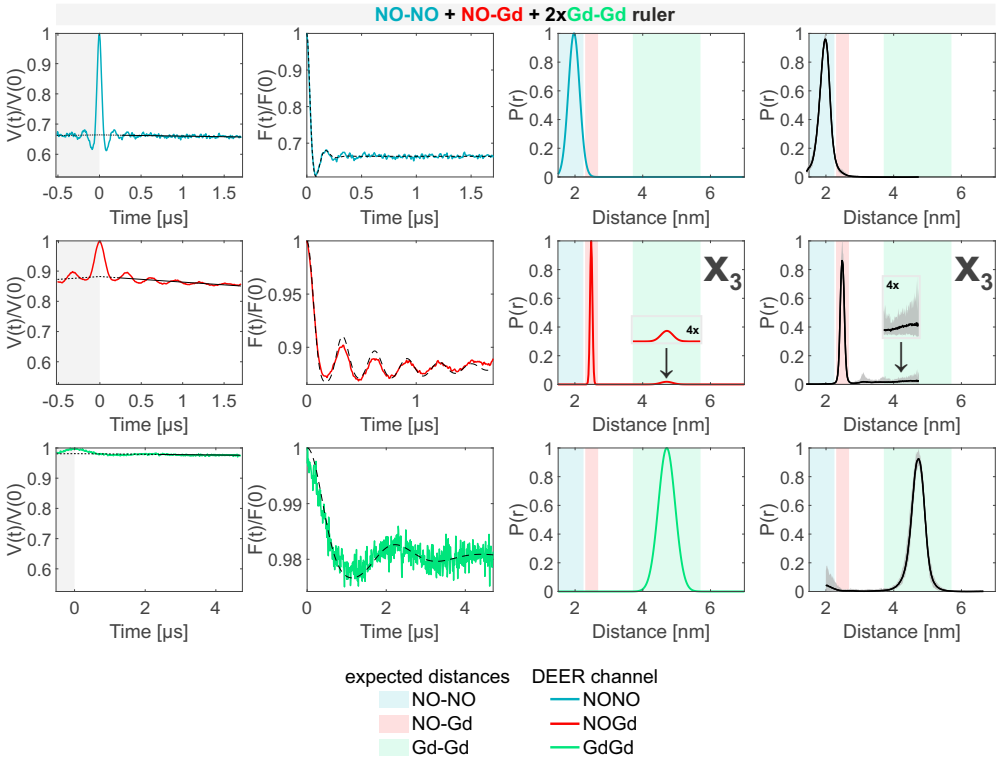

Figure 8. ~~Mixture of~~ Sample containing the NO-NO, NO-Gd and Gd-Gd rulers mixed in a 1:1:2 ratio. The ~~DEER setup~~ legend is ~~introduced in Fig. 3. Left, primary data with background fit (gray areas are excluded from data evaluation); middle, form factors with Gaussian fit; right, obtained distance distributions. Color coding~~ the same as in Fig. 4. "$\mathbf{X}_3$" is a Gd-Gd crosstalk ~~signals~~ signal in the NOGd DEER channel in presence of a NO-Gd distance.

~~The~~ the NO-Gd crosstalk signal in the NONO channel $\mathbf{X}_1$ ~~is unavoidable when probing the NONO DEER channel at Q band~~ at 50 K (see Fig. ~~3(a)) in presence of a NO-Gd distance. There are two possible origins for this crosstalk signal of the NO-Gd ruler: i) the observer pulses selectively excite the NO and the pump pulse excites the NO and sub-optimally the coupled Gd spins ; ii)the observer pulses excite the NO and sub-optimally the Gd while~~ 4(c) and 7) lies in the excitation of the ~~pump pulse selectively excites the coupled NO spins . To test the effect of the pump pulse on the crosstalk signal, we decreased its power by 12 dB in order to optimize the pump~~ Gd spins with a pump pulse close to 4π (see Fig. 2(b)) while optimally observing the NO spins and/or in the excitation of the NO spins with an optimal pump π-pulse ~~for~~ while sub-optimally observing the Gd spins. ~~This resulted only in a small decrease in the modulation depth of the crosstalk signal (data not shown) which implies that there are contributions of Gd spins both in the pump and in the observer echo at the same time. Subsequently, both possibilities discussed above occur simultaneously.~~ We could not find ~~a~~ an experimental strategy to minimize this crosstalk signal~~in the NONO channel, however, if~~ . However, when the NO-NO ruler (therefore a real NO-NO distance) is present, the contribution of this unwanted signal was found to be negligible due to the shorter phase memory time of the NO in the NO-Gd ruler with

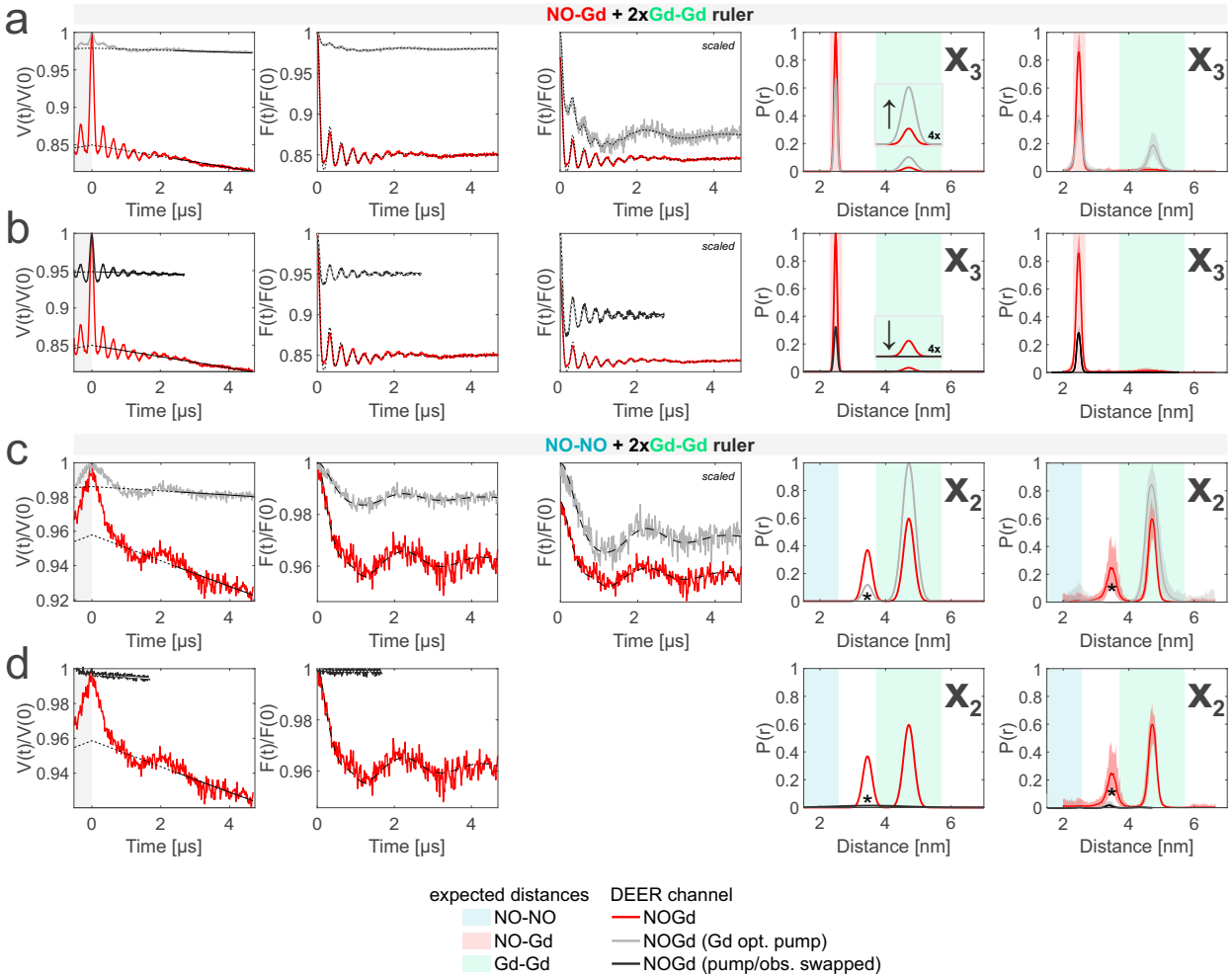

Figure 9. Crosstalk signal identification. First column, primary data with background fit (gray areas are excluded from data evaluation); second column, form factors with fit obtained with Gaussian fitting routine; third column, form factors scaled to same modulation depth and offsetted by constant value; fourth column, obtained distance distributions; fith column, DeerNet analysis (Generic network) to provide an error estimation. (a-b) Sample containing the NO-Gd and the Gd-Gd rulers mixed in a 1:2 molar ratio (related to Fig. 7). The NOGd channel contains a Gd-Gd crosstalk signal in presence of a NO-Gd distance ($\mathbf{X}_3$). (a) Decreasing the pump pulse power in the standard NOGd DEER setup (see Fig. 3(b)) from optimally pumping NO (red) to optimally pumping the Gd (-12 dB, gray) changes the signal-to-crosstalk ratio and thereby allows to identify the crosstalk signal. (b) By pumping the Gd and observing on the NO (swapped NOGd DEER setup, see Fig. 3(d)) the Gd-Gd crosstalk signal can be fully removed from the NOGd DEER channel (black). (c-d) Sample containing the NO-NO and the Gd-Gd rulers mixed in a 1:2 molar ratio (related to Fig. 6). The NOGd DEER channel contains a Gd-Gd crosstalk signal in absence of a NO-Gd distance ($\mathbf{X}_2$). The distance indicated with an asterisk originates from a spectrometer-specific artifact signal. (c) Analogous to (a). (d) Analogous to (b).

respect of the NO in the NO-NO ruler, and due to the presence of an additional NO signal contribution in the observer echo which is not dipolarly coupled to the Gd spins (see Fig. 5 ~~(a))~~and 8).

~~Crosstalk signal identification. Left, primary data with background fit (gray areas are excluded from data evaluation); middle, form factors with Gaussian fit (original data and modulation depth scaled data); right, obtained distance distributions. Color coding as in Fig. 4. In the NOGd DEER setup, NO is pumped and Gd is observed as illustrated in Fig. 3(b). Both $\mathbf{X}_2$ and $\mathbf{X}_3$ crosstalk signals arise from a partial excitation of the underlying Gd at the NO position in an NOGd DEER. (a) and (b) show how decreasing the pump pulse power from optimally pumping NO (red) to optimally pumping Gd (-12 dB, dark red) changes the signal-to-crosstalk ratio and thereby allowing the identification of the crosstalk signal. The relative change in modulation depth is considerably larger if a "real" NO-Gd signal is present together with the crosstalk signal ($\approx$ 1/7x for $\mathbf{X}_3$ versus $\leq$ 1/2x for $\mathbf{X}_2$). The 3.5 nm distance marked with an asterisk originates from a spectrometer-specific artifact.~~

~~We focus now on~~ Fig. 9(a,b) provides identification and suppression strategies for the $\mathbf{X}_3$ crosstalk signal (Gd-Gd crosstalk in the NOGd channel in the presence of a real NO-Gd distance) from Fig. ~~5(c). In Fig. 7 (a) we present a long NOGd DEER time trace (red) detected on the sample from Fig. 5(c). The two distinct dipolar frequencies of the NO-Gd (high frequency) and Gd-Gd (low frequency) rulers are clearly visible in the primary data. The distance analysis of this time trace using two Gaussians reveals both an NO-Gd distance peak and a Gd-Gd crosstalk distance peak. Since in the NOGd DEER channel, NO is pumped and Gd is observed~~ 7 and 8. In our NOGd DEER setup (see Fig. 3(b)), the observer pulses excite only Gd spins, therefore, the Gd-Gd crosstalk signal originates from sub-optimally pumping the Gd at the NO position due to the spectral overlap. ~~Decreasing the pump pulse power~~ In Fig. 9(a) we present a strategy to identify this crosstalk signal by lowering the power of the pump pulse at the NO position by 12 dB~~from optimally pumping the NO with a π-pulse to optimally pumping the Gd with a π-pulse (dark red in~~ , in order to increase the contribution of the Gd-Gd dipolar frequency in the time trace and to simultaneously suppress the modulation depth of the NO-Gd frequencies. In red we present the NOGd DEER time trace with the distance distributions extracted by Gaussian fitting and DeerNet from Fig. 7 ~~(a)) strongly~~ and in gray the time trace obtained with a pump pulse of 12 dB less power. Decreasing the power of the pump pulse decreases the modulation depth by a factor of 7 (from 15% to 2%~~; $\approx$ 1/7x~~) and changes the ratio of the ~~two distance peaks~~ modulation depths of the two dipolar frequencies (and of the extracted distance peaks) in favor of the crosstalk ~~distance~~signal, as expected (see arrow in the inset). ~~The~~ Therefore, the 12 dB decrease in power ~~of the pump pulse~~ allows the identification of the $\mathbf{X}_3$-crosstalk signal since ~~optimally pumping the Gd~~ it promotes the intensity of the Gd-Gd crosstalk distance ~~(see next paragraph for additional information)~~ while strongly decreasing the intensity of the NO-Gd distance. ~~It is important to note that also~~ Notably, the Gd-optimized pump pulse with 12 dB less power still partially pumps the NO and therefore the DEER trace contains a residual NO-Gd signal contribution.

~~In~~ Fig. ~~7~~9(b) ~~the same approach is used to identify the Gd-Gd crosstalk signal~~ presents a strategy to completely suppress this crosstalk signal by swapping the pump and observer positions in the NOGd channel ~~in the absence of a NO-Gd signal ($\mathbf{X}_2$) ((~~see Fig. ~~5~~3(b) ~~). The NO-Gd signal (red) is a superposition of the Gd-Gd crosstalk signal corresponding to a distance centered at 4.7 nm and an additional 3.5 nm distance originating from a spectrometer-specific artifact. Decreasing the pump pulse power by 12 dB to optimally pumping the Gd (dark red) considerably suppresses the spectrometer-specific artifact contribution while~~

slightly decreasing the main Gd-Gd dipolar modulation. The modulation depth contribution of the Gd-Gd signal in this setup is about 1.25%, which is in line with the modulation depth obtained with the same setup on the isolated Gd-Gd ruler shown in Fig. S2 (SI Part B). Therefore, we found that by changing the pump power by 12 dB to optimize the inversion pulse for the Gd spins, the modulation depth of the Gd-Gd signal slightly decreases. We can conclude that if there is a Gd-Gd crosstalk signal in the NOGd channel in the absence of a real NO-Gd signal, decreasing the pump power by 12 dB produces a small change in modulation depth ($\leq$ 1/2x versus (d)). This makes it possible to identify an $\mathbf{X}_2$ crosstalk signal. In contrast, if a real NO-Gd distance is present, as in the case of the $\mathbf{X}_3$ crosstalk signal in Fig. 7(a), the overall modulation depth largely decreases (to $\approx$ 1/7x) and the ratio of the distance peaks in the overall distance distribution changes in favor of the crosstalk peak, which can be identified.

Crosstalk signal suppression. The absolute values of the complex FSE spectra detected using a refocused Hahn echo sequence (DEER observer sequence) on the 1:2 mixture of the NO-Gd and Gd-Gd ruler are shown. The experiments were performed at 10 K with a shot repetition time of 100 ms (filtering for the NO, see Fig. 2). With respect to the standard NOGd DEER setup shown in Fig. 3(b), the positions of pump and observer pulses were exchanged. The observer was placed at a frequency where 100% pulse amplitude corresponds to a π-pulse on the NO. Due to the distinct transition moments of NO and Gd, the relative intensities of the spectral contributions change when varying the pulse amplitudes. At 50% amplitude only the NO spectrum is refocused.

To actually suppress crosstalk signals in the overall distance distribution, swapping the pump and observer positions in the NOGd channel could be an option. Usually we pump the NO and observe strategy has already proven to be effective in a case study (Shah et al., 2019). Usually, the NO spins are pumped and the Gd spins are observed (see Fig. 3(b)) to optimize the modulation depth in the NOGd channel. In this setup, the observer echo is solely created by the Gd spins. Therefore, crosstalk signals are caused by the pump pulse which is optimized to selectively address NO spins but also partially excites Gd spins. If the positions of the pump and observer pulses are swappedexchanged, the observer pulses will be are placed in the spectral overlapregion of the spectral overlap at the spectral maximum of the NO, while the pump pulse will excite only Gd spins. The advantage of the latter approach swapped setup is that the observer sequence being composed of three pulses can act as a better filter for one spin species than a single pump pulse. This is illustrated in Fig. 8 where field-swept echo experiments were performed at different pulse amplitudes using the refocused echo created by the DEER observer sequence (in absence of the pump pulse). At 100% pulse amplitude, the pulses are optimal The observer sequence uses $\pi/2$- and π-pulses optimized by nutation experiments for the NO , but strongly over-flipping the Gd spins, for which optimal π-pulses require an amplitude of approximately 14% (both determined via transient nutation experiments, data not shown). By lowering the pulse amplitude of the observer pulses to 50%, it is possible to favor even more the intensity of the NO spins in the refocused echo with respect to the signal, which will overflip the Gd spins, therefore increasing the selectivity of the observer sequence towards the wanted NO spins and suppressing the Gd contribution . Using these pulse amplitudes decreasing their contribution in the observer sequence should maximize the wanted NO-Gd signal, while minimizing the unwanted Gd-Gd crosstalk signalecho. The main disadvantage of this approach is that very the long shot repetition times are time required to observe on the NO (100 ms for the NO with respect to 1 ms for Gd in the conventional setup at 10 K), which makes DEER data acquisition impractically

longfor this combination of spin labels to achieve a satisfactory signal-to-noise. Additionally, the small fraction of Gd spins excited by a Gaussian pump leads to a small modulation depth modulation depth will be smaller for the desired NO-Gd signal. The latter issue could be improved using phase- frequency- and amplitude-modulated broadband pump pulses, as it was previously shown as a way to improve modulation depths for Gd spin pairs (Doll et al., 2013; Spindler et al., 2013; Doll et al., 2015; Bahrenberg et al., 2017). Overall, this approach is interesting and might be of use for other pairs of orthogonal spin labels. In Fig. 9(b) we present in red the NOGd DEER time trace with the distance distributions extracted by Gaussian fitting and DeerNet from Fig. 7; in black the time trace obtained with a swapped NOGd DEER setup (see Fig. 3(d)) recorded at 30 K. To achieve a sufficient signal-to-noise ratio in a reasonable measuring time, we increased the temperature to shorten the longitudinal relaxation time of the NO, thereby enabling the use of a faster srt. Notably, to maintain the polarization introduced by the pump pulse, the longitudinal relaxation time of the pumped Gd spins needs to remain longer than the dipolar evolution time of the DEER sequence. We found that at 50 K, which is the temperature commonly used in NONO DEER, the T_1 of Gd is too short (see Table S3, SI Part B). The best compromise between the T_1 of the Gd and of the NO spins is found at 30 K for the investigated samples (see Fig. S3, SI Part B). The time trace detected at 30 K (black in Fig. 9(b)) shows a dipolar frequency with a modulation depth of 5%, characteristic of the pure NOGd signal. Therefore, the GdGd crosstalk signal could be fully suppressed in the NOGd channel using the swapped setup at 30 K maintaining a good signal-to-noise ratio.

In principle, it is also possible to optimize the power of the pulses to further improve the selectivity of the observer sequence towards the NO, as shown in Fig. S10 (SI Part B) for the 10 K case.

4 Conclusions and outlook

In this work we thoroughly investigated the appearance of crosstalk signals between the three possible DEER channels at Q-band frequencies on mixtures of NO-NO, NO-Gd and Gd-Gd rulers with non-overlapping distance distributions. Crosstalk signals in DEER experiments with two types of spin systems had been suspected in the literature before (Gmeiner et al., 2017a; Teucher et a but could never be unambiguously identified and characterized.

We experimentally detected a NO-Gd crosstalk signal $\mathbf{X}_1$ in the NONO DEER channel in In Fig. 9(c,d) we show the effects of the absence of real NO-NO distances and two 12 dB power decrease in the pump (identification strategy) and of the swapped setup (suppression strategy) on the Gd-Gd crosstalk signals $\mathbf{X}_2$ or $\mathbf{X}_3$, signal detected in the NOGd DEER channel in the absence and presence of a real of a NO-Gd distance, respectively. We theoretically predicted a fourth crosstalk signal $\mathbf{X}_4$ (see Table S2)which describes a signal ($\mathbf{X}_2$) from Fig. 6. Decreasing the pump pulse power by 12 dB (gray trace in Fig. 9(c)) decreases the dipolar modulation of the Gd-Gd crosstalk in the NONO channel that was not experimentally detected. This is most likely due to : the low modulation depth that would be expected for this signal based on the non-perfect pump and observer pulses; the long Gd-Gd distance of 4.7 nm of the chosen ruler , which makes it more difficult to identify signals with very low modulation depth; the low spectral density of the Gd at signal (and diminishes the impact of the spectrometer artifact) with respect to the position of the NO; and the large modulation depth of a real red trace (taken from Fig. 6). The modulation depth contribution of the Gd-Gd signal in this setup is about 1.25%, which is in line with the modulation depth obtained with the

same setup on the isolated Gd-Gd ruler under the same experimental conditions shown in Fig. S11 (SI Part B). Unfortunately, this is not a good strategy to identify such crosstalk signals. However, in line with the conclusion drawn above, using the swapped setup at 30 K removed the dipolar frequency of the Gd-Gd signal in the NOGd DEER channel, thereby suppressing the unwanted crosstalk signal.

4 Conclusions and outlook

In this work we thoroughly investigated the appearance of crosstalk signals between three DEER channels at Q-band frequencies with mixtures of NO-NO~~signal if present~~, NO-Gd and Gd-Gd rulers.

Our experimental findings ~~confirm~~ further corroborate the notion that crosstalk signals can be expected in ~~4-pulse DEER experiments performed with the observer and/or pump pulses positioned in the region of spectral overlap between NO and Gd spins.Therefore,NONO and NOGd DEER experiments are prone to crosstalk signals, while~~ the NONO and NOGd DEER channels with the setups presented in Fig. 3(a,b). In contrast, the GdGd DEER ~~channel with the setup suggested here is intrinsically crosstalk-free (see~~ setup in Fig. 3(c) ~~).~~

is crosstalk-free. All detected crosstalk signals are of experimental relevance when ~~orthogonally-labeled biomolecular complexes~~ biomolecular complexes labeled with NO and Gd are investigated, since they are in the order of 10% of the maximally expected modulation depth in the respective DEER channel~~for a doubly spin-labeled protein with 100% labeling efficiency. Signals of this strength are easily resolvable by state-of-the-art high-power Q-band spectrometers (Polyhach et al., 2012) and therefore~~. Therefore, they entail the risk of data misinterpretation when unknown mixtures of orthogonally-labeled proteins are studied. Notably, ~~we found that if a real NO-NO dipolar oscillation with a large modulation depth is present in the NONO channel and the stoichiometric~~ the relative strengths of the crosstalk signals depend on the molar ratio of the different ~~spin types is similar, the possible~~ types of spin labels. Additionally, other factors such as relative labeling efficiencies, widths of the peaks in the distance distribution, presence of long distances close to detection limit etc. may also modulate the impact of the crosstalk signals in the distance analysis.

The NO-Gd crosstalk ~~signal is negligible~~ in the NONO channel ($\mathbf{X}_1$) was found to be negligible if a real NO-NO dipolar oscillation is present, due to the dominating signal contribution from the NO spins which are not dipolarly coupled to Gd spins and to the larger modulation depth of the real signal (in the order of 30 - 40%) with respect to the ~~expected 1~~2 - ~~2% of~~ 4% expected for the crosstalk signal.

We were not able to find a suitable spectroscopic approach to identify ~~the NO-Gd crosstalk signal in the NONO channel (~~or suppress $\mathbf{X}_1$~~)~~, apart from an identification strategy based on the comparison of the distance distributions ~~detected with~~ in the NONO and NOGd DEER channels on the same sample, which can be ambiguous. ~~Therefore, if a dipolar oscillation is detected in the NONO DEER channel and the obtained distance distribution overlaps with the one detected in the NOGd channel, further analysis is required. To clarify whether~~ A possible method to clarify the presence of a crosstalk signal is ~~detected, we propose~~ to prepare an analogous sample ~~with the Gd-labeled proteins exchanged with the unlabeled variants~~without the Gd labels. If the NONO DEER channel is free of dipolar oscillations, the signal previously detected ~~signal was a~~ was a NOGd crosstalk

signal; otherwise, if the same dipolar frequency is detected, ~~then it was~~ it can be concluded that it is a real NO-NO distance. In principle, based on the spectral overlap, we also expected a Gd-Gd crosstalk in the NONO channel ($\mathbf{X}_4$), but this signal could not be experimentally detected, possibly due to its negligible modulation depth.

~~For~~ We found that the Gd-Gd crosstalk signals in the NOGd DEER channel ~~, which~~ are the most relevant unwanted signals in ~~the~~ terms of their relative modulation depths with respect to the desired NO-Gd signals. Therefore, their presence can be detrimental in the analysis of complex protein mixtures~~, we propose an~~ . We propose a quick identification strategy based on decreasing the power of the pump pulse positioned at the maximum of the nitroxide spectrum by 12 dB to optimally pump the Gd spins. This ~~allows to unambiguously identify crosstalk signals $\mathbf{X}_2$ and $\mathbf{X}_3$ via relative changes in their modulation depth. If the overall modulation depth decreases only marginally (maximally to ≈50% of its initial value), the DEER signal is caused by Gd-Gd crosstalk and no real NO-Gd distances are present. In contrast, if the modulation depth decreases to ≈15% of its original value and the primary time trace differs, then the signal is a mixture of a~~ method changes the relative intensities of the crosstalk Gd-Gd and the real NO-Gd ~~signal and a Gd-Gd crosstalk signal. In this case, the crosstalk signal is oftype~~signals, thereby only allows identification of $\mathbf{X}_3$ ~~and there must be a relative increase in intensity of the crosstalk signal with respect to the real signal contribution in the distance distribution. This change in relative intensities aids the identification of the crosstalk signal. Notably, the exact values of the relative changes of the modulation depths presented here are valid only in our experimental setup and need to be calibrated for each setup using standard samples. Swapping~~ . Most importantly, we show that Gd-Gd crosstalk signals can be completely suppressed by swapping the position of the pump and observer pulses in the NOGd DEER channel ~~was found to be in principle promising to suppress the NO-Gd crosstalk signal, but experimentally impracticable for samples containing NO and Gd spins due to the prohibitively long shot repetition time of the experiment and the small modulation depths expected~~at 30 K (setup in Fig. 3(d)). This swapped setup suffers from low modulation depths and long acquisition times. Broadband excitation pump pulses may alleviate the small modulation depth issue for spins with large zero field splittings and the ~~long acquisition times would benefit if faster relaxing spin 1/2 labels are used~~acquisition time can be shortened by going to higher temperatures, if possible, or by using faster relaxing NO labels.

It ~~is important to note that the relative strengths of the crosstalk signals depend on the relative molar ratio of the different types of spin labels, as shown by a complete set of experiments performed on an independent set of samples with mixtures of the rulers in equimolar quantities (Table S3 and Fig. S3 to S5, SI Part B). Additionally, other experimental properties such as the relative modulation depths of the real signals and the relative widths of the distance distributions may modulate the relevance of the crosstalk signals in the overall data analysis. Therefore, in this work we identified possible problems arising from crosstalk signals in three DEER channels when using NO and Gd mixtures, but the extent of the crosstalk signals and their relevance on data interpretation depends on the specific properties of the sample under investigation.~~

would be insightful to use a multi-frequency approach to find the best-suited frequency for each DEER channel and spin label combination. However, Q band ~~currently offers the highest sensitivity to perform the~~ can be currently considered as the best compromise in frequency to perform all three-channel DEER experiments with ~~samples containing both NO and Gd spin labels on a commercial spectrometer. Gd spin labels would gain in sensitivity at higher frequencies thanks to the~~ high sensitivity. In fact, Q band is superior to X band for NONO DEER (Polyhach et al., 2012). W band would allow gaining

in sensitivity for GdGd DEER gains thanks to a narrowing of the ~~spectrum, however, the broadening of the NO spectrum would probably counterbalance these effects in the NONO and NOGd DEER channels. In general, it would be insightful to have a multi-frequency approach and perform these types of experiments at Q- andW-band or higher frequencies to find the best-suited frequency band for each DEER channel- and label- combination. The use of an AWG is advantageous for the proposed identification strategy due to the possibility to use Gaussian pulses (Teucher and Bordignon, 2018), which remove residual "2+1" pulse train signals increasing signal fidelity and to further explore additional benefits of broadband excitation pulses. We did not analyze the effects of multispin systems with more than 2 spins in the mixture, but we can anticipate that appearance of ghost peaks (von Hagens et al., 2013) will further complicate data analysis and additional experiments with one type of label removed at a time from the sampleshould be planned.~~

~~Combinations of other orthogonal spin labels with spectral overlap will be also prone to crosstalk signals in DEER and we foresee that the approaches suggested here to identify and possibly suppress unwanted crosstalk signal should be applicable~~Gd spectrum (Goldfarb, 2014). However, at W band, NOGd DEER requires dedicated homemade dual mode resonators for an optimal positioning of the pump and observer pulses (Tkach et al., 2011; Kaminker et al., 2013). Additionally, the g anisotropy of the NO spectrum is fully resolved at W band, whereby pump pulses will excite less NO spins, creating lower modulation depths, and, most importantly, orientation selection will have to be taken into account to obtain the correct distance distributions (see for example (Polyhach et al., 2007)). A large variety of spectroscopically distinguishable spin label pairs is readily available and will be more often used in the future to investigate complex biomolecular systems owing to the inceased information content that can be obtained from a single sample. Since most spin labels are non-perfectly orthogonal, the methods of identification and suppression of crosstalk signals proposed here can aid to increase DEER signal fidelity in future applications.

Author contributions. MT and EB designed the research. MT prepared the EPR samples and performed all EPR experiments. Compound design and synthesis was contributed by MQ, NC, HH, and AG. MT and EB discussed the results and wrote the manuscript. MQ and AG wrote the SI Part A. The manuscript was revised by all authors.

Competing interests. The authors declare no competing interests.

Acknowledgements. EB and MT would like to thank Laura Galazzo and Svetlana Kucher for the DEER analysis of the artifact signal and for fruitful discussions. We acknowledge support by Deutsche Forschungsgemeinschaft (DFG, German Research Foundation) under Germany's Excellence Strategy – EXC-2033 – Projektnummer 390677874 (EB), the DFG Priority Program SPP1601 "New Frontiers in Sensitivity in EPR Spectroscopy" [DFG BO 3000/2-1 (EB); DFG GO 555/6-2 (AG)], DFG BO 3000/5-1 (EB), DFG INST 130/972-1 FUGG (EB) and SFB958 – Z04 (EB). The Q-band resonator was kindly gifted by G. Jeschke (ETH Zürich/Switzerland).

References

Abdullin, D., Duthie, F., Meyer, A., Müller, E. S., Hagelueken, G., and Schiemann, O.: Comparison of PELDOR and RIDME for distance measurements between nitroxides and low–spin Fe (III) ions, J. Phys. Chem. B, 119, 13 534–13 542, 2015.

Ackermann, K., Pliotas, C., Valera, S., Naismith, J. H., and Bode, B. E.: Sparse labeling PELDOR spectroscopy on multimeric mechanosensitive membrane channels, Biophys. J., 113, 1968–1978, 2017.

Akhmetzyanov, D., Plackmeyer, J., Endeward, B., Denysenkov, V., and Prisner, T.: Pulsed electron–electron double resonance spectroscopy between a high-spin Mn2+ ion and a nitroxide spin label, Phys. Chem. Chem. Phys., 17, 6760–6766, 2015.

Altenbach, C.: LongDistances, http://www.biochemistry.ucla.edu/Faculty/Hubbell/, accessed August 31, 2020.

Bahrenberg, T., Rosenski, Y., Carmieli, R., Zibzener, K., Qi, M., Frydman, V., Godt, A., Goldfarb, D., and Feintuch, A.: Improved sensitivity for W-band Gd (III)-Gd (III) and nitroxide-nitroxide DEER measurements with shaped pulses, J. Magn. Reson., 283, 1–13, 2017.

Bode, B. E., Plackmeyer, J., Prisner, T. F., and Schiemann, O.: PELDOR measurements on a nitroxide-labeled Cu (II) porphyrin: orientation selection, spin-density distribution, and conformational flexibility, The Journal of Physical Chemistry A, 112, 5064–5073, 2008.

Bode, B. E., Plackmeyer, J., Bolte, M., Prisner, T. F., and Schiemann, O.: PELDOR on an exchange coupled nitroxide copper (II) spin pair, Journal of Organometallic Chemistry, 694, 1172–1179, 2009.

Brandon, S., Beth, A. H., and Hustedt, E. J.: The global analysis of DEER data, Journal of magnetic resonance, 218, 93–104, 2012.

Chiang, Y.-W., Borbat, P. P., and Freed, J. H.: The determination of pair distance distributions by pulsed ESR using Tikhonov regularization, J. Magn. Reson., 172, 279–295, 2005.

Doll, A., Pribitzer, S., Tschaggelar, R., and Jeschke, G.: Adiabatic and fast passage ultra-wideband inversion in pulsed EPR, J. Magn. Reson., 230, 27–39, 2013.

Doll, A., Qi, M., Wili, N., Pribitzer, S., Godt, A., and Jeschke, G.: Gd (III)–Gd (III) distance measurements with chirp pump pulses, J. Magn. Reson., 259, 153–162, 2015.

Edwards, T. H. and Stoll, S.: Optimal Tikhonov regularization for DEER spectroscopy, Journal of Magnetic Resonance, 288, 58–68, 2018.

Ezhevskaya, M., Bordignon, E., Polyhach, Y., Moens, L., Dewilde, S., Jeschke, G., and Van Doorslaer, S.: Distance determination between low-spin ferric haem and nitroxide spin label using DEER: the neuroglobin case, Mol. Phys., 111, 2855–2864, 2013.

Galazzo, L., Meier, G., Timachi, M. H., Hutter, C. A., Seeger, M. A., and Bordignon, E.: Spin-labeled nanobodies as protein conformational reporters for electron paramagnetic resonance in cellular membranes, PNAS, 117, 2441–2448, 2020.

Garbuio, L., Bordignon, E., Brooks, E. K., Hubbell, W. L., Jeschke, G., and Yulikov, M.: Orthogonal Spin Labeling and Gd (III)–nitroxide distance measurements on bacteriophage T4-lysozyme, J. Phys. Chem. B, 117, 3145–3153, 2013.

Gmeiner, C., Dorn, G., Allain, F. H., Jeschke, G., and Yulikov, M.: Spin labelling for integrative structure modelling: A case study of the polypyrimidine-tract binding protein 1 domains in complexes with short rnas, Phys. Chem. Chem. Phys., 19, 28 360–28 380, 2017a.

Gmeiner, C., Klose, D., Mileo, E., Belle, V., Marque, S. R., Dorn, G., Allain, F. H., Guigliarelli, B., Jeschke, G., and Yulikov, M.: Orthogonal tyrosine and cysteine site-directed spin labeling for dipolar pulse EPR spectroscopy on proteins, J. Phys. Chem, 8, 4852–4857, 2017b.

Goldfarb, D.: Gd 3+ spin labeling for distance measurements by pulse EPR spectroscopy, Physical Chemistry Chemical Physics, 16, 9685–9699, 2014.

Ibáñez, L. F. and Jeschke, G.: Optimal background treatment in dipolar spectroscopy, Phys. Chem. Chem. Phys., 22, 1855–1868, 2020.

Jassoy, J. J., Berndhäuser, A., Duthie, F., Kühn, S. P., Hagelueken, G., and Schiemann, O.: Versatile trityl spin labels for nanometer distance measurements on biomolecules in vitro and within cells, Angew. Chem., 56, 177–181, 2017.

Jeschke, G.: DEER distance measurements on proteins, Ann. Rev. Phys. Chem., 63, 419–446, 2012.

Jeschke, G.: The contribution of modern EPR to structural biology, Emerg. Top. Life Sci., 2, 9–18, 2018.

Jeschke, G., Chechik, V., Ionita, P., Godt, A., Zimmermann, H., Banham, J., Timmel, C., Hilger, D., and Jung, H.: DeerAnalysis2006—a comprehensive software package for analyzing pulsed ELDOR data, Appl. Magn. Reson., 30, 473–498, 2006.

Jeschke, G., Sajid, M., Schulte, M., and Godt, A.: Three-spin correlations in double electron–electron resonance, Phys. Chem. Chem. Phys., 11, 6580–6591, 2009.

Jeschke, G., Sajid, M., Schulte, M., Ramezanian, N., Volkov, A., Zimmermann, H., and Godt, A.: Flexibility of shape–persistent molecular building blocks composed of p-phenylene and ethynylene units, J. Am. Chem. Soc., 132, 10 107–10 117, 2010.

Joseph, B., Tormyshev, V. M., Rogozhnikova, O. Y., Akhmetzyanov, D., Bagryanskaya, E. G., and Prisner, T. F.: Selective High-Resolution Detection of Membrane Protein–Ligand Interaction in Native Membranes Using Trityl–Nitroxide PELDOR, Angew. Chem., 55, 11 538–11 542, 2016.

Junk, M. J., Spiess, H. W., and Hinderberger, D.: DEER in biological multispin-systems: a case study on the fatty acid binding to human serum albumin, Journal of Magnetic Resonance, 210, 210–217, 2011.

Kaminker, I., Yagi, H., Huber, T., Feintuch, A., Otting, G., and Goldfarb, D.: Spectroscopic selection of distance measurements in a protein dimer with mixed nitroxide and Gd 3+ spin labels, Phys. Chem. Chem. Phys., 14, 4355–4358, 2012.

Kaminker, I., Tkach, I., Manukovsky, N., Huber, T., Yagi, H., Otting, G., Bennati, M., and Goldfarb, D.: W-band orientation selective DEER measurements on a Gd3+/nitroxide mixed-labeled protein dimer with a dual mode cavity, J. Magn. Reson., 227, 66–71, 2013.

Kaminker, I., Bye, M., Mendelman, N., Gislason, K., Sigurdsson, S. T., and Goldfarb, D.: Distance measurements between manganese (II) and nitroxide spin-labels by DEER determine a binding site of Mn2+ in the HP92 loop of ribosomal RNA, Phys. Chem. Chem. Phys., 17, 15 098–15 102, 2015.

Lueders, P., Jeschke, G., and Yulikov, M.: Double electron-electron resonance measured between Gd3+ ions and nitroxide radicals, J. Phys. Chem. Lett., 2, 604–609, 2011.

Lueders, P., Jäger, H., Hemminga, M. A., Jeschke, G., and Yulikov, M.: Distance measurements on orthogonally spin-labeled membrane spanning WALP23 polypeptides, J. Phys. Chem. B, 117, 2061–2068, 2013.

Martin, R. E., Pannier, M., Diederich, F., Gramlich, V., Hubrich, M., and Spiess, H. W.: Determination of end-to-end distances in a series of TEMPO diradicals of up to 2.8 nm length with a new four-pulse double electron electron resonance experiment, Angew. Chem., 37, 2833–2837, 1998.

Meyer, A. and Schiemann, O.: PELDOR and RIDME measurements on a high-spin manganese (II) bisnitroxide model complex, J. Phys. Chem. A, 120, 3463–3472, 2016.

Meyer, A., Abdullin, D., Schnakenburg, G., and Schiemann, O.: Single and double nitroxide labeled bis (terpyridine)-copper (II): Influence of orientation selectivity and multispin effects on PELDOR and RIDME, Phys. Chem. Chem. Phys., 18, 9262–9271, 2016.

Milov, A., Salikhov, K., and Shirov, M.: Use of the double resonance in electron spin echo method for the study of paramagnetic center spatial distribution in solids, Fizika Tverdogo Tela, 23, 975–982, 1981.

Milov, A., Ponomarev, A., and Tsvetkov, Y. D.: Electron-electron double resonance in electron spin echo: Model biradical systems and the sensitized photolysis of decalin, Chem. Phys. Lett., 110, 67–72, 1984.

Motion, C. L., Lovett, J. E., Bell, S., Cassidy, S. L., Cruickshank, P. A., Bolton, D. R., Hunter, R. I., El Mkami, H., Van Doorslaer, S., and Smith, G. M.: DEER sensitivity between iron centers and nitroxides in heme-containing proteins improves dramatically using broadband, high–field EPR, J. Phys. Chem. Lett., 7, 1411–1415, 2016.

Narr, E., Godt, A., and Jeschke, G.: Selective measurements of a nitroxide–nitroxide separation of 5 nm and a nitroxide–copper separation of 2.5 nm in a terpyridine-based copper (II) complex by pulse EPR spectroscopy, Angew. Chem., 41, 3907–3910, 2002.

Pannier, M., Veit, S., Godt, A., Jeschke, G., and Spiess, H. W.: Dead-time free measurement of dipole–dipole interactions between electron spins, J. Magn. Reson., 142, 331–340, 2000.

Plitzko, J. M., Schuler, B., and Selenko, P.: Structural biology outside the box—inside the cell, Curr. Opin. Struct. Biol., 46, 110–121, 2017.

Polyhach, Y., Godt, A., Bauer, C., and Jeschke, G.: Spin pair geometry revealed by high-field DEER in the presence of conformational distributions, Journal of Magnetic Resonance, 185, 118–129, 2007.

Polyhach, Y., Bordignon, E., Tschaggelar, R., Gandra, S., Godt, A., and Jeschke, G.: High sensitivity and versatility of the DEER experiment on nitroxide radical pairs at Q-band frequencies, Phys. Chem. Chem. Phys., 14, 10 762–10 773, 2012.

Pribitzer, S., Sajid, M., Hülsmann, M., Godt, A., and Jeschke, G.: Pulsed triple electron resonance (TRIER) for dipolar correlation spectroscopy, J. Magn. Reson., 282, 119–128, 2017.

Qi, M., Hülsmann, M., and Godt, A.: Spacers for geometrically well–defined water–soluble molecular rulers and their application, J. Org. Chem., 81, 2549–2571, 2016a.

Qi, M., Hülsmann, M., and Godt, A.: Synthesis and Hydrolysis of 4–Chloro–PyMTA and 4–Iodo–PyMTA Esters and Their Oxidative Degradation with Cu(I/II) and Oxygen, Synthesis, 48, 3773–3784, 2016b.

Ritsch, I., Hintz, H., Jeschke, G., Godt, A., and Yulikov, M.: Improving the accuracy of Cu (ii)–nitroxide RIDME in the presence of orientation correlation in water-soluble Cu (ii)–nitroxide rulers, Phys. Chem. Chem. Phys., 21, 9810–9830, 2019.

Schmidt, T., Wälti, M. A., Baber, J. L., Hustedt, E. J., and Clore, G. M.: Long Distance Measurements up to 160 Å in the GroEL Tetradecamer Using Q-Band DEER EPR Spectroscopy, Angew. Chem., 55, 15 905–15 909, 2016.

Schweiger, A. and Jeschke, G.: Principles of pulse electron paramagnetic resonance, Oxford University Press, 2001.

Shah, A., Roux, A., Starck, M., Mosely, J. A., Stevens, M., Norman, D. G., Hunter, R. I., El Mkami, H., Smith, G. M., Parker, D., and Lovett, J. E.: A gadolinium spin label with both a narrow central transition and short tether for use in double electron electron resonance distance measurements, Inorg. Chem., 58, 3015–3025, 2019.

Shevelev, G. Y., Krumkacheva, O. A., Lomzov, A. A., Kuzhelev, A. A., Trukhin, D. V., Rogozhnikova, O. Y., Tormyshev, V. M., Pyshnyi, D. V., Fedin, M. V., and Bagryanskaya, E. G.: Triarylmethyl labels: toward improving the accuracy of EPR nanoscale distance measurements in DNAs, J. Phys. Chem. B, 119, 13 641–13 648, 2015.

Spindler, P. E., Glaser, S. J., Skinner, T. E., and Prisner, T. F.: Broadband inversion PELDOR spectroscopy with partially adiabatic shaped pulses, Angew. Chem., 52, 3425–3429, 2013.

Stein, R. A., Beth, A. H., and Hustedt, E. J.: A Straightforward approach to the analysis of double electron–electron resonance data, in: Meth. Enzymol., vol. 563, pp. 531–567, Elsevier, 2015.

Stoll, S. and Schweiger, A.: EasySpin, a comprehensive software package for spectral simulation and analysis in EPR, J. Magn. Reson., 178, 42–55, 2006.

Tait, C. E. and Stoll, S.: Coherent pump pulses in double electron electron resonance spectroscopy, Phys. Chem. Chem. Phys., 18, 18 470–18 485, 2016.

Teucher, M. and Bordignon, E.: Improved signal fidelity in 4-pulse DEER with Gaussian pulses, J. Magn. Reson., 296, 103–111, 2018.

Teucher, M., Zhang, H., Bader, V., Winklhofer, K. F., García-Sáez, A. J., Rajca, A., Bleicken, S., and Bordignon, E.: A new perspective on membrane-embedded Bax oligomers using DEER and bioresistant orthogonal spin labels, Sci. Rep., 9, 1–15, 2019.

Tkach, I., Sicoli, G., Höbartner, C., and Bennati, M.: A dual-mode microwave resonator for double electron–electron spin resonance spectroscopy at W-band microwave frequencies, Journal of Magnetic Resonance, 209, 341–346, 2011.

Tschaggelar, R., Kasumaj, B., Santangelo, M. G., Forrer, J., Leger, P., Dube, H., Diederich, F., Harmer, J., Schuhmann, R., García-Rubio, I., et al.: Cryogenic 35GHz pulse ENDOR probehead accommodating large sample sizes: Performance and applications, J. Magn. Reson., 200, 81–87, 2009.

Valera, S., Ackermann, K., Pliotas, C., Huang, H., Naismith, J. H., and Bode, B. E.: Accurate extraction of nanometer distances in multimers by pulse EPR, Chem.: Eur. J., 22, 4700–4703, 2016.

von Hagens, T., Polyhach, Y., Sajid, M., Godt, A., and Jeschke, G.: Suppression of ghost distances in multiple-spin double electron–electron resonance, Phys. Chem. Chem. Phys., 15, 5854–5866, 2013.

Worswick, S. G., Spencer, J. A., Jeschke, G., and Kuprov, I.: Deep neural network processing of DEER data, Sci. Adv., 4, eaat5218, 2018.

Wu, Z., Feintuch, A., Collauto, A., Adams, L. A., Aurelio, L., Graham, B., Otting, G., and Goldfarb, D.: Selective distance measurements using triple spin labeling with Gd3+, Mn2+, and a nitroxide, J. Phys. Chem, 8, 5277–5282, 2017.

Yulikov, M.: Spectroscopically orthogonal spin labels and distance measurements in biomolecules, EPR, 24, 1–31, 2015.

Yulikov, M., Lueders, P., Warsi, M. F., Chechik, V., and Jeschke, G.: Distance measurements in Au nanoparticles functionalized with nitroxide radicals and Gd 3+–DTPA chelate complexes, Phys. Chem. Chem. Phys., 14, 10 732–10 746, 2012.